An Ab Initio Study of Complexes With N-H-N Hydrogen Bonds

by

Barry C. Husowitz

Submitted in Partial Fulfillment of the Requirements

For the Degree of

Master of Science

in the

Chemistry

Program

YOUNGSTOWN STATE UNIVERSITY

August, 2002

An Ab Initio Study of Complexes With N-H-N Hydrogen Bonds

Barry C. Husowitz

I hereby release this thesis to the public. I understand this thesis will be made available from the OhioLINK ETD Center and the Maag Library Circulation Desk for public access. I also authorize the University or other individuals to make copies of this thesis as needed for scholarly research.

Signature:

Barry C. Husowitz, Student — 6/01/02 Date

Approvals:

Dr. Janet E. Del Bene, Thesis Advisor — 6/06/02 Date

Dr. Howard Mettee, Committee Member — 6/6/02 Date

Dr. Timothy Wagner, Committee Member — 6/6/02 Date

Dr. Peter J. Kasvinsky, Dean of Graduate Studies — 6/11/02 Date

ABSTRACT

Ab initio MP2/6-31+G(d,p) calculations have been performed on a series of hydrogen-bonded complexes stabilized by N-H-N hydrogen bonds. These complexes have 2,5- and 3,4-disubstituted pyrroles as proton donors (with substituents H, F, and Be^{+1}), and nitrogen bases including HCN, LiCN, NaCN, SCN^-, OCN^-, NH_3, and $N(CH_3)_3$ as proton acceptors. Correlations have been established among the structures, binding energies, proton-stretching frequencies, and intensities of the proton-stretching bands of these complexes. The great majority of complexes are stabilized by traditional N-H...N hydrogen bonds, with proton-shared and ion-pair hydrogen bonds occurring only in charged complexes.

ACKNOWLEDGEMENTS

I would like to thank my advisor, Dr. Janet E. Del Bene, for her guidance on this project. I am proud to have studied under her. I am grateful for the knowledge she has imparted to me. This knowledge will benefit me for years to come. I am also grateful for the time she has dedicated, and for her patience and understanding. Secondly, I would like to thank the National Science Foundation (NSF) for financial support of this research, and the Ohio Supercomputer Center. Finally, I would like to thank my family and friends for believing in me, and for their constant encouragement throughout my life. This has made it possible for me to make it this far. I would especially like to thank my brother for his encouraging words and constant support.

TABLE OF CONTENTS

LIST OF FIGURES

LIST OF TABLES

I. INTRODUCTION:

Hydrogen bonding is an important intermolecular interaction, which is ubiquitous in chemical and biochemical systems. Hydrogen bonding influences the properties of water in its various phases and of molecules in aqueous solution. The high boiling points of many solvents are a consequence of hydrogen bonding, and hydrogen bond formation influences products formed in reactions.[1] In biological systems such as DNA, the formation of nucleic acid base pairs involves hydrogen bonding.[2] Hydrogen bonds determine the structures of proteins[3], and are a factor in enzymatic activity.[4] It has been postulated that low barrier hydrogen bonds can provide stabilization during enzyme catalysis, which results in rate enhancement of the reaction.[4]

In the most general case the hydrogen bond can be represented as

A-H---B

where A-H is the proton donor and B is the proton acceptor atom. In recent studies, three types of hydrogen bonds have been characterized: traditional, ion-pair, and proton-shared.[5-7] In a traditional hydrogen bond between two neutral molecules, the A-H covalent bond of the proton donor remains intact in the complex. If proton transfer from A to B occurs, an ion-pair hydrogen bond is formed. In this type of hydrogen bond a covalent bond is now formed between H^+ and B, and what was previously the proton acceptor is now the proton donor. Intermediate between traditional and ion-pair hydrogen bonds is the proton-shared hydrogen bond. In this type of hydrogen bond the A—B distance is shorter than in traditional and ion-pair hydrogen bonds, but the A-H and B-H bond lengths are longer than the covalent A-H and B-H^+ bonds in traditional and ion-pair hydrogen bonds, respectively.

The first ab initio theoretical studies of hydrogen-bonded complexes were conducted in the late 1960's and the early 1970's.[8-12] In these studies a single determinant Hartree-Fock wavefunction was used with a small basis set. Geometry optimizations where carried out by freezing the monomer geometries and optimizing the intermolecular distance and intermolecular angles. The intermolecular coordinates were varied cyclicly and independently until convergence criteria were met. It was not until the 1980's that computationally efficient algorithms were developed for obtaining first and second derivatives of the energy with respect to the nuclear coordinates. The derivatives where first evaluated numerically, but later analytically.[13-20] As a result, automated full geometry optimizations can now be easily carried out. The availability of analytical derivatives also permits routine calculation of harmonic infra-red (IR) spectra.

An important experimental method for studying hydrogen-bonded complexes is IR spectroscopy. The IR spectra of hydrogen-bonded complexes are characterized by a shift to lower frequency of the A-H proton-stretching band compared to that of the corresponding monomer, and by a dramatic increase in the intensity of this band.[7,21-23] Ab initio calculations of vibrational spectra can help experimentalists gain insight into the properties of hydrogen-bonded complexes. Many ab initio calculations on various hydrogen-bonded complexes and their IR spectra have been performed.[7,22,24,25]

Previous studies of hydrogen-bonded complexes that are most closely related to those investigated in this project were carried out by Del Bene, Person, and Szczepaniak on complexes between 4-substituted pyridines and hydrogen halides.[5,6] These complexes are represented as

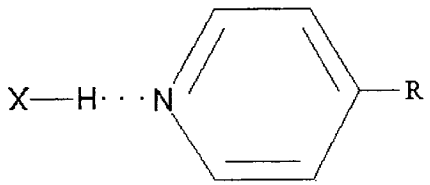

where R represents the substituents Be^+, CN, F, Cl, H, CH_3, NH_2, Li, Na, S^- and O^-, and X is a halogen atom. The complexes were optimized at the MP2/6-31+G(d,p) level of theory. In this study computed structures and vibrational spectroscopic properties were related to acid and base strength and hydrogen bond type.

Figure 1 shows the computed spectra for the ClH:4-R-pyridine complexes. The spectra are arranged in order of increasing proton affinity of the substituted pyridine. The complexes of ClH:4-R-pyridines with R=CN, F, Cl, H, CH_3 and NH_2 are stabilized by traditional hydrogen bonds, and a single strong Cl-H stretching band appears in the computed harmonic spectra, with frequencies ranging from 2524 cm^{-1} to 2156 cm^{-1}. For these complexes, as the proton affinity of the 4-substituted pyridine increases, the Cl-N distance decreases, the Cl-H distance increases, the binding energy (ΔE) increases, and the frequency (ν) of the Cl-H stretching band decreases.

The complexes of ClH:4-Li-pyridine and ClH:4-Na-pyridine are stabilized by proton-shared hydrogen bonds. These complexes have very short Cl-N distances. Several strong bands appear in the computed spectra of these two complexes, with frequencies ranging from 1700 to 600 cm^{-1}. The multiple bands are due to coupling of the Cl-H stretching mode to ring vibrational modes.

As the proton affinity of the base increases further, proton transfer occurs in the complexes ClH:4-S^-- pyridine and ClH:4-O^--pyridine. The Cl-N distance and the proton-stretching frequency increase relative to complexes with proton-shared hydrogen bonds,

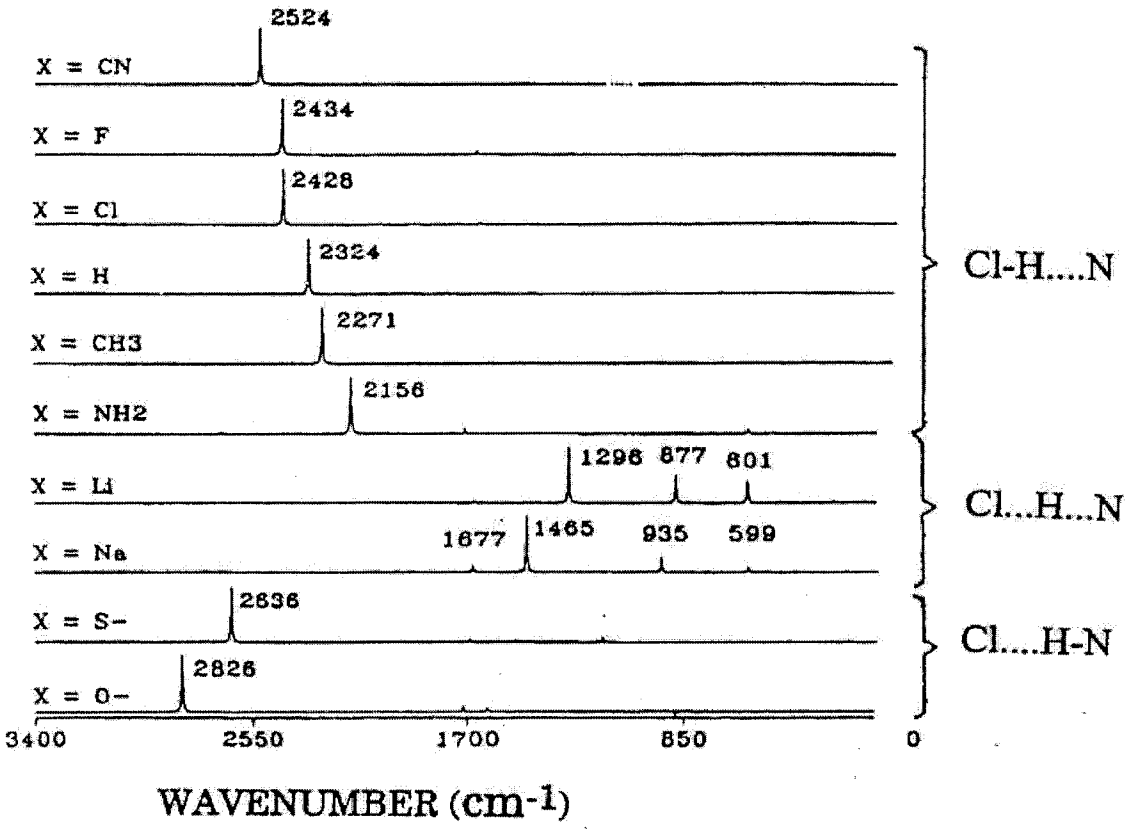

Figure 1: Computed harmonic vibrational spectra of ClH:4-R-pyridine complexes, from reference 6.

and the N-H distance continues to decrease. The single strong band in the IR spectra corresponds to an N-H^+ stretch, shifted downfield relative to the corresponding pyridinium ion.

In related studies, Del Bene and Jordan examined hydrogen-bonded complexes between hydrogen halides as proton donors and NH_3 and $N(CH_3)_3$ as proton acceptors.[26,27] Examples of traditional, proton-shared and ion-pair hydrogen bonds were found. Systematic studies such as those reported for complexes with hydrogen halides have not been carried out on complexes with N-H-N hydrogen bonds. Therefore, in this project hydrogen-bonded complexes of pyrrole and substituted pyrroles with various nitrogen bases will be investigated. The proton-donating ability and proton-accepting ability of the hydrogen-bonded pair will be systematically varied by chemical substitution in an attempt to span the three hydrogen bond types.

Ab initio calculations on isolated pyrrole have been carried out, and optimized structures and harmonic vibrational spectra were reported.[28,29] The only study of hydrogen-bonded complexes with pyrrole was reported by Jiang and Tsai.[30] These authors obtained structures and harmonic vibrational frequencies for pyrrole:HF complexes using second-order Møller-Plesset perturbation theory and density functional theory with various basis sets.

Aims of Study:

The current ab initio study focuses on N—H—N hydrogen bonds. Therefore in this work complexes with pyrroles and disubstituted pyrroles as proton donors to a series of nitrogen bases will be investigated. The complexes can be represented as

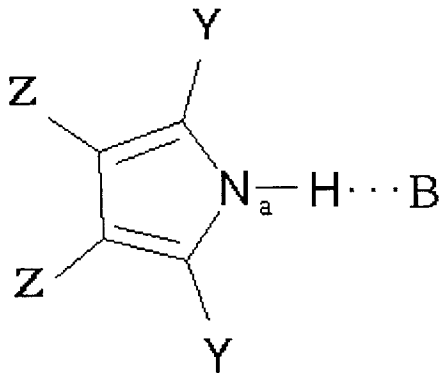

where Y may be H, F, or Be^+ and Z is H, giving 2,5-disubstituted pyrroles; or Z is H, F, or Be^+ and Y is H, giving 3,4-disubstituted pyrroles. The nitrogen bases B are HCN and its derivatives, LiCN, NaCN, SCN^-, and OCN^-, as well as NH_3 and $N(CH_3)_3$.

The specific aims of this work are

1. to systematically vary the proton-donating and proton-accepting abilities of the hydrogen-bonded pair in an attempt to span the three hydrogen bond types;
2. to determine the optimized MP2/6-31+G(d,p) structures of the monomers and complexes;
3. to calculate the harmonic vibrational spectra of monomers and complexes at the same level of theory;
4. to examine the effect of hydrogen bonding on the frequency and intensity of the proton-stretching band;
5. to correlate structural and spectroscopic properties with binding energies and hydrogen bond type;

6. to determine whether proton-shared or ion-pair hydrogen bonds can be formed in neutral complexes with N-H-N hydrogen bonds.

II. METHODS:

In order to calculate the electronic energy and electron distribution of a molecule, the wavefunction Ψ must be known. Both the energy E, and the wavefunction Ψ, can be obtained by solving the nonrelativistic time-independent Schrödinger equation

$$H\Psi = E\Psi \tag{1}$$

where H is the Hamiltonian operator. The Hamiltonian is defined as

$$H = T + V \tag{2}$$

where T is the kinetic energy operator and V the potential energy operator. The Hamiltonian operator in atomic units for n electrons in a field of m fixed nuclei is written as[31-33]

$$H = -\frac{1}{2}\sum_{i}^{n}\nabla_i^2 + \sum_{i<j}^{n}\sum^{n}\frac{1}{r_{ij}} - \sum_{i}^{n}\sum_{A}^{m}\frac{Z_A}{r_{iA}} + \sum_{A<B}^{m}\sum^{m}\frac{Z_A Z_B}{R_{AB}} \tag{3}$$

where the first term is the kinetic energy operator, and the remaining terms are the terms of the potential energy operator including the repulsion between each pair of electrons, the nuclear-electron attraction, and the nuclear-nuclear repulsion, respectively. The

Schrödinger equation can be solved exactly only for the hydrogen atom or any one-electron system. However, the results of this exact solution, namely the hydrogen atomic orbitals, are useful as a starting point for calculating the electronic distribution of other atoms and molecules which have more than one electron.[33,34]

In this study, ab initio calculations will be performed to determine Ψ and E. Ab initio means, "from first principles", that is, using only the fundamental constants and the atomic numbers of the nuclei, with no other adjustable parameters or data from experiment. However, within the ab initio framework it is necessary to choose a basis set to describe the atomic orbitals, and a wavefunction model. These will now be discussed in general, and the wavefunction model and basis set that will be used in this study will be identified.

Basis sets:

A basis set is a set of mathematical functions that describe orbitals on atoms. Basis sets are of three general types: minimal, split-valence, and augmented. A minimal basis set contains one basis function to describe each orbital of an atom in the valence shell and below. The advantage of using a minimal basis set is that the number of coefficients to be determined variationally is small, and this reduces the computational problem. However, the disadvantages are that the number of basis functions is not proportional to the number of electrons, anisotropic molecular environments are not correctly represented, and polarization effects are usually not well-described.[31]

An improvement over a minimal basis set is a double-zeta (DZ) or triple-zeta (TZ) basis set. In a DZ basis set, each orbital in the valence shell and below is

represented by two basis functions, while for a TZ basis set each orbital is replaced by three basis functions. These basis sets are now twice and three times larger than a minimal basis set, respectively, and this increases the computational task.

A valence double-split basis set is a DZ basis for orbitals in the valence space, but only a single basis function for each orbital below the valence shell. Similarly, a valence triple-split basis set is a TZ basis set for the valence shell, but has only one basis function per inner shell orbital. The most popular double-split valence basis set used as a starting point to construct larger basis sets is the 6-31G basis set,[31] which contains one set of inner shell functions for each atomic orbital below the valence shell, and two sets of valence shell atomic functions. For example, for C, the 6-31G basis set has one function to describe the inner shell 1s orbital, and two sets of s and p functions to describe the valence shell. The notation 6-31G means 6 gaussian functions are used to describe each inner shell function, 3 gaussians are used to describe each valence shell orbital in the first set, and 1 gaussian is used for each function in the second set. However, these basis functions are still severely limited.[22,31]

In a molecular environment atomic orbitals are distorted and polarized due to the formation of bonds. To account for this nonuniform displacement of charge away from the nuclear center, basis functions are added with angular momentum quantum number ℓ one greater than the maximum value found in the valence shell. For carbon this means adding a set of d orbitals (ℓ=2), and for hydrogen a set of p orbitals (ℓ=1). The newly added functions are called polarization functions, and are required to describe anisotropic environments. Adding polarization functions to the 6-31G basis set gives 6-31G(d,p),

where one set of six Cartesian d functions are added to each nonhydrogen atom, and one set of p functions to each H atom.

Further basis set improvements are made by adding diffuse functions. These are important for describing negatively charged species, lone pairs of electrons, and π electrons[31]. The diffuse basis functions are of s and p type for nonhydrogen atoms, and s for hydrogen. They have exponents that are considerably smaller than the other valence basis functions and provide a better description of electron density far removed from the nuclear centers. The notation for basis sets augmented with diffuse functions is a "+" symbol for diffuse functions on heavy atoms, and "++" for diffuse functions on hydrogen as well. Thus, the 6-31+G(d,p) basis set is an augmented valence double-split basis set with polarization functions on all atoms and diffuse functions on nonhydrogen atoms.

Wavefunction models:

Before discussing the wavefunction model in detail it is important to note that electrons have spin ($+\frac{1}{2}$ or $-\frac{1}{2}$), and that electron spin must be incorporated into Ψ. The spin angular momentum is represented by a vector **s** that has the components of s_x, s_y and s_z. Since these components follow the commutation relations of general angular momentum, only s^2, the magnitude of the vector s and one other component (s_x, s_y or s_z) can be determined simultaneously. The z-axis component is normally chosen as this component. Thus, a one-electron wavefunction must describe both space and spin coordinates. If ψ_j (i) describes the spatial coordinates of electron i, the spin coordinate is described by[31,33]

$$S_z\,\alpha(i) = +\frac{1}{2}\hbar\,\alpha(i) \tag{4}$$

$$S_z\,\beta(i) = -\frac{1}{2}\hbar\,\beta(i) \tag{5}$$

where $\hbar=\frac{h}{2\pi}$ and S_z is the operator of the spin angular momentum component along the z-axis. The many-electron wavefunction Ψ must also be an eigenfunction of the many-electron spin operators S^2 and S_z, whose eigenrelations may be written as[33]

$$S^2\,\Psi = S(S+1)\Psi \tag{6}$$

$$S_z\ \Psi = M_s\,\Psi \tag{7}$$

where M_s is the sum of the individual spin eigenvalues (m_s).

$$M_s = \sum_i^n m_s \tag{8}$$

S, the total resultant spin angular momentum, may have any positive half-integral value (0, ½, 1, 3/2,....), and M_s is the component of S along the z-axis. For a given resultant spin S there are 2S+1 possible M_s values. The quantity (2S+1) is the multiplicity. Thus for total S=0, the multiplicity is one (singlet, nondegenerate state). For S=1/2, (2S+1) is 2 (doublet, doubly-degenerate state), for S=1, 2S+1 is 3, (triplet, triply-degenerate state), and so forth.

The total wavefunction Ψ must describe both the space and spin coordinates of all the electrons, and must satisfy two requirements. The first requirement is that Ψ must be

antisymmetric. Antisymmetry means that if two electrons are interchanged, then the wavefunction must change sign. The second requirement is that the Pauli exclusion principle must be obeyed. This means that no two electrons can be assigned to identical spinorbitals. These two conditions are most easily satisfied if the wavefunction is represented as a determinant, specifically the Slater determinant, which for an n-electron system with n even and no orbital degeneracies, is

$$\Psi(1,2,\ldots,n) = (n!)^{-1/2} \begin{vmatrix} \psi_1(1) & \bar{\psi}_1(1) & \psi_2(1) & \bar{\psi}_2(1) & \ldots\ldots\ldots & \psi_{n/2}(1) & \bar{\psi}_{n/2}(1) \\ \psi_1(2) & \bar{\psi}_1(2) & \psi_2(2) & \bar{\psi}_2(2) & \ldots\ldots\ldots & \psi_{n/2}(2) & \bar{\psi}_{n/2}(2) \\ \ldots\ldots & \ldots\ldots & \ldots\ldots & \ldots\ldots & \ldots\ldots & \ldots\ldots & \ldots\ldots \\ \psi_1(n) & \bar{\psi}_1(n) & \psi_2(n) & \bar{\psi}_2(n) & \ldots\ldots\ldots & \psi_{n/2}(n) & \bar{\psi}_{n/2}(n) \end{vmatrix} \quad (9)$$

where ψ_i (a) represents the spinorbital

$$\psi_i(a) = \psi_i(a)\alpha(a) \quad (10)$$

and $\bar{\psi}_i$ (a) represents the spinorbital

$$\bar{\psi}_i(a) = \psi_i(a)\,\beta(a) \quad (11)$$

In the Slater determinant the first row assigns electron one to all the possible spinorbitals, while the second row assigns electron two to all possible spinorbitals, and so forth. Each column assigns all electrons to a given spinorbital. Thus, the Slater determinant satisfies the Pauli-Exclusion Principle, since if two rows or two columns are identical then the

determinant is zero. It also maintains antisymmetry, since if rows i and j are interchanged the sign of the determinant changes.

In order to obtain the best single-determinant wavefunction Ψ, the Hartree-Fock method is used.[31-34] The Hartree-Fock method is a variational method used to determine a set of molecular orbitals (MOs) in terms of a linear combination of atomic orbitals (the LCAO approximation). The LCAO approximation can be written as

$$\psi_i = \sum_{\mu=1}^{p} c_{\mu i} \varphi_\mu \tag{12}$$

where ψ_i is the molecular orbital, $c_{\mu i}$ are the expansion coefficients, and $\varphi_1, \varphi_2, \ldots, \varphi_p$ are the atomic basis functions. The expansion coefficients $c_{\mu i}$ are determined by the variational method, which minimizes the energy E with respect to the coefficients $c_{\mu i}$.

$$\frac{d < E >}{d c_{\mu i}} = 0 \tag{13}$$

In carrying out a Hartree-Fock calculation, an initial set of coefficients is chosen and used to construct the Fock matrix. This matrix is diagonalized, and a new set of coefficients is obtained. This process is repeated until the coefficients from two consecutive iterations are identical to within a given tolerance. The Hartree-Fock method is a self-consistent field (SCF) method, which means that the molecular orbitals are derived from their own effective potential. The Hartree-Fock energy is the lowest energy that can be obtained from a single determinant wavefunction with a given nuclear configuration and basis set.[31-34] It is guaranteed to be an upper bound to the exact energy.

Moreover, the Hartree-Fock wavefunction is size-consistent, which means that if a system of several molecules is infinitely separated, the energy computed at infinite separation is equal to the sum of these energies computed for the isolated molecules.[22,31,32,34]

The most severe limitation of the Hartree-Fock method is that it describes an average (SCF) potential for the electrons.[31-34] The model does not properly consider instantaneous interaction between electrons. This is a particular problem for two electrons in the same orbital, which on average are too close to each other. As a result, the Hartree-Fock energy is always too high. The difference between the Hartree-Fock energy and the true energy of the system is referred to as the electron correlation error.

There has been a great effort in quantum chemistry to improve the Hartree-Fock wavefunction and energy by explicitly treating the electron correlation problem. The most rigorous and straightforward way of doing this is through configuration interaction. In a configuration interaction (CI) treatment, the wavefunction Φ is written as[32,34]

$$\Phi = c_0 \Psi^0 + \sum_{i,a} c_i^a \Psi_i^a + \sum_{\substack{i \le j \\ a \le b}} c_{ij}^{ab} \Psi_{ij}^{ab} + \sum_{\substack{i \le j < k \\ a \le b < c}} c_{ijk}^{abc} \Psi_{ijk}^{abc} + \ldots\ldots \qquad (14)$$

where Ψ^0 is the Hartree-Fock reference wavefunction, Ψ_i^a represents all possible excitations from orbital i which is doubly occupied in Ψ^0 to unoccupied (virtual) orbital a, Ψ_{ij}^{ab} represents all possible two-electron excitations, Ψ_{ijk}^{abc} all three electron excitations, and so forth. The expansion coefficients are again determined variationally. If all possible n-electron excitations are included, the resulting wavefunction Φ is a full CI wavefunction, which is the exact solution of the Schrödinger equation with a given basis

set. Unfortunately, full CI calculations are feasible only for extremely small molecules or molecular ions.[22,31,32,34] Therefore, in practice, it is necessary to approximate the full CI wavefunction in some way.

The most commonly used methods for obtaining correlated wavefunctions are CI truncated to singles and doubles (CISD), coupled cluster (CC) theory, and Møller-Plesset perturbation theory truncated to some order n (MPn).

CISD is a computationally feasible method for moderate size systems, is variational, but is not size consistent.[22,31,32,34] For hydrogen-bonded complexes this is a significant problem since it yields incorrect binding energies. In fact, the computed binding energy is often positive, which means that the complex is not bound at all. Therefore, the CISD method is not recommended for hydrogen-bonded systems.[22]

The second method is the coupled cluster (CC) method in which the Hamiltonian is written in exponential form.[32] There are various levels of CC theory, including coupled cluster singles and doubles (CCSD); CCSD(T), which includes non-iterative triples; CCSDT which includes full triples, and CCSDTQ, which includes triples and quadruples. Because of the exponential ansatz, CC methods are size consistent, but they are not variational. CC methods are most reliable, but are computationally demanding and therefore not feasible for large systems such as those that will be investigated in this work.[22,32]

In Møller-Plesset (MP) theory, correlation effects are treated as a perturbation using many-body perturbation theory. Møller-Plesset theory is widely used to investigate hydrogen-bonded complexes, since it is size consistent.[22,31,32,34] However, MP calculations are not variational, and the MP expansion may converge slowly.

In Møller-Plesset perturbation theory the generalized electronic Hamiltonian is written as[31]

$$\hat{H}_\lambda = \hat{H}_0 + \lambda\hat{V} \tag{15}$$

where $\hat{H}_0$ is the unperturbed Hamiltonian, and the perturbation $\lambda\hat{V}$, is defined by

$$\lambda\hat{V} = \lambda(\hat{H} - \hat{H}_0) \tag{16}$$

$\hat{H}$ is the correct Hamiltonian and λ is a dimensionless parameter. The unperturbed or zero Hamiltonian $\hat{H}_0$ is taken to be the sum of the one-electron Fock operators. The exact or full CI wavefunction (Ψ_λ) and energy (E_λ) may be written in powers of λ.

$$\Psi_\lambda = \Psi^{(0)} + \lambda\Psi^{(1)} + \lambda^2\Psi^{(2)} + \ldots\ldots \tag{17}$$

$$E_\lambda = E^{(0)} + \lambda E^{(1)} + \lambda^2 E^{(2)} + \ldots. \tag{18}$$

In practical applications the parameter λ is set equal to 1, and the series truncated at various orders. The method used is referred to by the highest term considered. For instance, if the series is truncated after the second order correction, it is referred to as MP2, if it is truncated after third order it is MP3, and so forth. The first terms in the expansion are[31]

$$\Psi^{(0)} = \Psi_0 \tag{19}$$

$$E^{(0)} = \sum_{i}^{occ} \varepsilon_i \tag{20}$$

$$E^{(0)} + E^{(1)} = \int \cdots \int \Psi_0 \hat{H} \Psi_0 \, d\tau_1 \, d\tau_2 \cdots d\tau_n \tag{21}$$

where Ψ_0 is the Hartree-Fock wavefunction, $E^{(0)}$ is the Hartree-Fock energy, and ε_i are the one-electron energies of the occupied molecular orbitals (ψ_i) at Hartree-Fock. Therefore, the MP energy to first order is the Hartree-Fock energy. The first-order contribution to the wavefunction is

$$\Psi^{(1)} = \sum_{s>0} (E_0 - E_s)^{-1} V_{so} \Psi_s \tag{22}$$

where E_s is the eigenvalue of a particular doubly-substituted determinant Ψ_s, while V_{so} are matrix elements of the perturbation operator $\hat{V}$, represented by

$$V_{so} = \int \cdots \int \Psi_s \hat{V} \Psi_0 \, d\tau_1 \, d\tau_2 \cdots d\tau_n \tag{23}$$

The integration is over all space and spin coordinates of the electrons. By Brillouin's theorem, the first-order energy corrections do not change the Hartree-Fock energy, since the Hamiltonian matrix elements between the Hartree-Fock wavefunction and singly-excited determinants are zero.

The second-order Møller-Plesset energy can be expressed as

$$E^{(2)} = -\sum_{i<j}^{occ} \sum_{a<b}^{virt} (\varepsilon_a + \varepsilon_b - \varepsilon_i - \varepsilon_j)^{-1} \left| (ij \,||\, ab) \right|^2 \tag{24}$$

where (ij || ab) is a two-electron integral over spin-orbitals defined by

$$(ij\,|\,|\,ab) = \int\int \psi_i^*(1)\,\psi_j^*(2)\,\left(\frac{1}{r_{12}}\right)[\,\psi_a(1)\,\psi_b(2) - \psi_b(1)\,\psi_a(2)\,]\,d\tau_1\,d\tau_2 \qquad (25)$$

and the integration is over all space and spin coordinates of the electrons.

Level of Theory for Studies of Hydrogen-bonded Complexes:

There have been many studies carried out on hydrogen-bonded complexes to establish what level of theory gives reliable structures and binding energies at minimal computational expense.[22,35-40] It has been shown that for hydrogen-bonded complexes, the MP energy expansion is dominated by the second-order term, while the third and fourth order contributions are small and may even be of opposite sign. Thus, MP2 with an appropriate basis set adequately describes the energy of hydrogen-bonded systems with minimal computational effort. The smallest basis set required is a split-valence basis set augmented with polarization functions on all atoms and diffuse functions on nonhydrogen atoms.[22,35-38] The MP2/6-31+G(d,p) level of theory has also been found to produce reliable structures and vibrational frequency shifts of the proton-stretching band in good agreement with experimental data, provided that anharmonicity corrections are not large.[7,22] Binding energies at this level are reasonable, but are usually too high. Improved energies require a larger basis set, and in some cases a better wavefunction.[22,35-40] In the current study, the MP2/6-31+G(d,p) level of theory will be used to determine structures, vibrational frequencies and binding energies. Although the binding energies may be too high, trends in binding energies in a closely related series of complexes have been shown to be reliable.[5,6,22]

Geometry Optimization:

The geometries of the monomers were fully optimized using the Gaussian 98[41] program at the MP2/6-31+G(d,p) level of theory. The nitrogen bases HCN, LiCN,

NaCN, SCN^- and OCN^- are linear, with $C_{\infty v}$ symmetry, and the bases NH_3 and $N(CH_3)_3$ have C_{3v} symmetry. Pyrrole and the 2,5- and 3,4-disustituted pyrroles have C_{2v} symmetry.

The complexes of pyrrole and the 2,5- and 3,4-disubstituted pyrroles with HCN, LiCN, NaCN, SCN^- and OCN^- were optimized at the MP2/6-31+G(d,p) level of theory under the constraint of C_{2v} symmetry. The complexes with NH_3 and $N(CH_3)_3$ have C_s symmetry, but local C_{2v} symmetry was imposed on pyrrole or the disubstituted pyrrole, and local C_{3v} symmetry on NH_3 and $N(CH_3)_3$. These restrictions maintain the linearity of the hydrogen bond. Vibrational frequencies were computed to verify that these optimized structures are equilibrium structures on their respective potential energy surfaces.

For selected complexes of pyrrole with NH_3 and $N(CH_3)_3$, two rotamers of C_s symmetry were optimized. In one rotamer, one hydrogen of NH_3 or one carbon of $N(CH_3)_3$ was placed in the plane of the pyrrole ring. In the second rotamer, the NH_3 or $N(CH_3)_3$ molecule was rotated 90 degrees from the previous conformation, so that one hydrogen or one carbon lies in the symmetry plane perpendicular to the plane of pyrrole. The rotational energy barrier for interconversion of the rotamers was found to be less than .01 kcal/mol, signifying that there is free rotation about the hydrogen bonding N-N axis.

For all complexes except those with NaCN as the proton acceptor, and all monomers except NaCN, the standard frozen core approximation was used. This approximation freezes all Hartree-Fock orbitals below the valence shell, which are then omitted from the correlation calculation. However, for complexes with NaCN as a base,

the standard option for freezing inner shell orbitals split degeneracies, or led to small energy gaps between frozen and active orbitals. To avoid these problems, only 1s orbitals were frozen in complexes with NaCN. This necessitated freezing only 1s orbitals in the NaCN monomer.

Calculation of Harmonic Vibrational Spectra:

Harmonic vibrational frequencies were calculated at the MP/6-31+G(d,p) level of theory to confirm equilibrium structures, to simulate IR spectra, and to obtain the zero-point vibrational energies necessary to evaluate binding enthalpies at 10 K. The harmonic vibrational calculations were done using the standard algorithms for computing analytical first and second-derivatives implemented in Gaussian 98.[41]

Harmonic vibrational calculations can be used to probe the vicinity of the minimum on the potential energy surface to determine whether a structure is a true minimum or a saddle point. If no imaginary frequencies exist, then the structure is a true minimum. If there are imaginary vibrational frequencies, then the optimized structure is a saddle point of order 1 if there is only one imaginary frequency, two if there are two imaginary frequencies, three if there are three imaginary frequencies, and so on. However, if the imaginary frequencies are small, then for the complexes investigated in this study, the optimized structures must be transition structures between two equivalent equilibrium structures, and the optimized structure is the vibrationally averaged structure. On the other hand, if the imaginary frequency is large, then the optimized structure is not close to the equilibrium structure, and a full optimization can yield significant geometry and energy changes.

Reaction Energies:

The reaction for the formation of a hydrogen-bonded complex can be written as

$$A\text{-}H(g) + B(g) \rightarrow A\text{-}H{:}B(g)$$

Since the vibrational spectra of hydrogen-bonded complexes are usually obtained in low temperature matrices (~10K), the reaction enthalpy at this temperature can be approximated as the enthalpy at 0K, and ΔH^0 may be written as

$$\Delta H^{10} \approx \Delta E_e^0 + \Delta E_v^0$$

where ΔE_e^0 is the electronic binding energy and ΔE_v^0 is zero-point energy contribution to ΔH^0. The electronic binding energy (ΔE_e^0) is the difference between the electronic energy of the hydrogen-bonded complex [E_e^0 (A-H:B)], and the electronic energies of the two monomers, E_e^0 (A-H) and E_e^0 (B).

$$\Delta E_e^0 = E_e^0 \text{ (A-H:B)} - E_e^0 \text{ (A)} - E_e^0 \text{ (B)} \qquad (29)$$

The zero point energy contribution ΔE_v^0, is evaluated as the difference between the zero-point energy of the hydrogen-bonded complex E_v^0 (A-H:B) and the zero-point energies of the isolated monomers, E_v^0 (A-H) and E_v^0 (B)

$$\Delta E_v^0 = E_v^0 \text{ (A-H:B)} - E_v^0 \text{ (A)} - E_v^0 \text{ (B)} \qquad (30)$$

To determine the basicities of the proton-acceptor molecules, the electronic proton affinity (PA) was evaluated at 0K. The protonation reaction can be written as

$$B(g) + H^+(g) \rightarrow B\text{-}H^+(g) \qquad (31)$$

The electronic energy of this reaction is

$$\Delta E_e^0 \text{ (PA)} = E_e^0(B\text{-}H^+) - E_e^0(B) \qquad (32)$$

where $E_e^0(B\text{-}H^+)$ is the electronic energy of the protonated base and $E_e^0(B)$ is the electronic energy of the base B. ΔE_e^0 (PA) for equation 32 is always negative. However,

since the proton affinity at 298K is defined as the negative energy ($-\Delta E_{PA}^{0}$) for reaction 31, the computed electronic proton affinities will be reported as positive numbers.

III. RESULTS and DISCUSSION:

The MP2/6-31+G(d,p) electronic energy (E_e^0), zero-point vibrational energy (E_v^0), equilibrium N_a-H distance [$R_e(N_a\text{-}H)$], proton-stretching frequency (ν) and intensity of the proton-stretching band (I) for pyrrole and disubstituted pyrroles are presented in Table 1. The N_a-H distances, frequencies, and intensities are given as reference data so that changes in these quantities due to hydrogen bonding can be seen. Pyrrole and the disubstituted pyrroles are listed in order of increasing acidity as determined by their binding energy to HCN.

Table 2 presents electronic energies (E_e^0), zero-point vibrational energies (E_v), and electronic proton affinities ($-\Delta E_{PA}^{0}$) of the nitrogen bases. The bases, HCN and its derivatives, are arranged in order of increasing basicity as evaluated from their electronic proton affinities. The bases NH_3 and $N(CH_3)_3$ are also listed in Table 2.

Table 3 presents the electronic energies, zero-point vibrational energies and imaginary frequency data for all of the complexes of pyrrole and disubstituted pyrroles with HCN and its derivatives that have been investigated in this study. An entry of "0" in the last column indicates that there are no imaginary frequencies. This means that the optimized structure is an equilibrium structure on the potential energy surface. There are some complexes listed in Table 3 that have small imaginary frequencies. The complexes pyrrole:NCS^-, pyrrole:NCO^-, 3,4-difluoropyrrole:NCS^-, 3,4-difluoropyrrole:NCO^-, 2,5-difluoropyrrole:$NCS^-$and 2,5-difluoropyrrole:NCO^- have a small imaginary frequency,

Table 1. MP2/6-31+G(d,p) electronic energies (E_e^0, amu), zero-point vibrational energies (E_v^0, kcal/mol), N_a-H distances (R_e, Å), harmonic proton-stretching frequencies (υ, cm^{-1}) and band intensities (I, km/mol) for pyrrole and disubstituted pyrroles

Monomer	E_e^0	E_v^0	$R_e(N_a\text{-}H)$	υ	I
Pyrrole	-209.53768	52.0	1.007	3735	80
3,4-difluoropyrrole	-407.55477	41.8	1.006	3745	110
2,5-difluoropyrrole	-407.55947	41.6	1.008	3730	149
2,5-diberylliumpyrrole^{+2}	-236.92122	40.8	1.012	3673	141
3,4-diberylliumpyrrole^{+2}	-236.92778	41.0	1.017	3620	295

Table 2. MP2/6-31+G(d,p) electronic energies (E_e^0, amu), zero-point vibrational energies (E_v^0, kcal/mol), and electronic proton affinities (ΔE_{PA}^0, kcal/mol) for the nitrogen bases

Monomer	E_e^0	E_v^0	$-\Delta E_{PA}^0$
HCN	- 93.17212	9.9	174.3
LiCN	-100.07104	4.3	228.5
NaCN	-254.46613	4.0	236.7
SCN^-	-490.29666	5.1	326.4
OCN^-	-167.69373	6.4	343.7
NH_3	- 56.39205	22.1	214.7
$N(CH_3)_3$	-173.91095	77.6	236.5

Table 3. MP2/6-31+G(d,p) electronic energies (E_e^0, amu), zero-point vibrational energies (E_v^0, kcal/mol), and frequency data for complexes of pyrrole and substituted pyrroles with HCN and its derivatives

Donor[a]	Acceptor	E_e^0	E_v^0	Imaginary frequencies[b]
Py	HCN	-302.71818	62.7	0
	LiCN	-309.62486	57.2	0
	NaCN	-464.02228	57.0	0
	SCN^{-1}	-699.86388	57.6	- 30[c], - 14[d]
	OCN^{-1}	-377.26720	58.9	- 20[c]
3,4-diFPy	HCN	-500.73713	52.5	0
	LiCN	-507.64592	47.0	0
	NaCN	-662.04392	46.8	0
	SCN^{-1}	-897.88985	47.3	- 31[c], - 14[d]
	OCN^{-1}	-575.29456	48.6	- 21[c]
2,5-diFPy	HCN	-500.74210	52.4	0
	LiCN	-507.65034	46.8	0
	NaCN	-662.04836	46.6	0
	SCN^{-1}	-897.89082	46.8	- 31[c]
	OCN^{-1}	-575.29598	47.7	- 24[c]
3,4-diBePy^{+2}	HCN	-330.13341	51.7	0
	LiCN	-337.07294	44.7	0
	NaCN	-491.48087	43.8	- 42[e]
	SCN^{-1}	-727.48058	43.8	-252[f], -214[g], -105[h]
	OCN^{-1}	-404.89957	45.5	-244[f], -238[g], -108[h]
2,5-diBePy^{+2}	HCN	-330.12815	51.7	- 31[i]
	LiCN	-337.07249	45.5	- 83[i]

a) Py = pyrrole
b) An entry of 0 means that there are no imaginary frequencies; frequencies in cm^{-1}.
c) Change of hybridization at the proton acceptor N coupled with pyrrole ring puckering out of the plane of pyrrole
d) Change of hybridization at the proton acceptor N coupled with an in-plane bending mode of the pyrrole ring
e) Ring puckering of the substituted pyrrole out of the plane
f) Change of hybridization at the proton acceptor N coupled with pyrrole ring puckering out of the plane of pyrrole
g) Change of hybridization at the proton acceptor N coupled with an in-plane bending mode of the pyrrole ring.
h) Ring puckering mode out of the plane of pyrrole
i) In-plane rotation of the substituted pyrrole due to strong interactions of Be^+ with the electron pair on the nitrogen of the proton acceptor

which corresponds to bending the proton acceptor out of the plane of the pyrrole ring, indicating a hybridization change of the nitrogen of NCO^- and NCS^-. This bending is coupled to a slight ring puckering of the pyrrole ring. The imaginary frequencies range from –31 cm^{-1} for 2,5-difluoropyrrole:NCS^- and 3,4-difluoropyrrole:NCS^-, to –20 cm^{-1} for pyrrole:NCO^-. The imaginary frequencies of –14 cm^{-1} for pyrrole:NCS^- and 3,4-difluoropyrrole:NCS^- correspond to an in-plane proton acceptor bend, also signifying a hybridization change of the NCS^- nitrogen. This motion is coupled to in-plane bending of the pyrrole ring. The imaginary frequency of –42 cm^{-1} for 3,4-diberylliumpyrrole:$NCNa^{+2}$ corresponds to an out-of-plane ring puckering of the pyrrole ring. As noted previously, structures with imaginary frequencies correspond to transition structures on the surface, but if the imaginary frequency is small, the optimized planar structure is the vibrationally averaged structure. Thus, complexes that have small imaginary frequencies (< 50 cm^{-1}) have been included in this work for comparative purposes.

The complexes of 3,4-diberylliumpyrrole:NCS^{+1} and 3,4-diberylliumpyrrole:NCO^{+1} have large imaginary frequencies, and these complexes have not been included in this study. The complexes 2,5-diberylliumpyrrole:NCH^{+2} and 2,5-diberylliumpyrrole:$NCLi^{+2}$ have imaginary frequencies corresponding to rotations that break the hydrogen bond and make Be^+ the electron pair acceptor. Thus, these two complexes have not been included in this work.

Table 4 reports the electronic energies, zero-point vibrational energies, and imaginary frequency data for complexes of pyrrole and disubstituted pyrroles with NH_3 and $N(CH_3)_3$. Except for 2,5-diberylliumpyrrole:$N(CH_3)_3^{+2}$, the single imaginary

Table 4: MP2/6-31+G(d,p) electronic energies (E_e^0, amu), zero-point vibrational energies (E_v^0, kcal/mol), and frequency data for complexes of pyrrole and disubstituted pyrroles with NH_3 and $N(CH_3)_3$.

Donor[a]	Acceptor	E_e^0	E_v^0	Imaginary frequencies[b]
Py	NH_3[c]	-265.94341	75.8	0
	NH_3[d]	-265.94341		
3,4-diFPy	NH_3[c]	-463.96290	65.6	- 18[e]
	NH_3[d]	-463.96290		
Py	$N(CH_3)_3$[c]	-383.46481	130.4	- 14[e]
	$N(CH_3)_3$[d]	-383.46481		
2,5-diFPy	NH_3[c]	-463.96952	65.4	- 7[e]
	NH_3[d]	-463.96951		
3,4-diFPy	$N(CH_3)_3$[c]	-581.48445	120.2	0
2,5-diBePy^{+2}	NH_3[c]	-293.34999	64.5	- 13[e]
	NH_3[d]	-293.34999		
2,5-diFPy	$N(CH_3)_3$[c]	-581.49261	119.9	0
3,4-diBePy^{+2}	NH_3[c]	-293.36161	64.0	0
	NH_3[d]	-293.36161		
2,5-diBePy^{+2}	$N(CH_3)_3$[c]	-410.88485	118.8	- 40[f], -12[e]
	$N(CH_3)_3$[d]	-410.88483		
3,4-diBePy^{+2}	$N(CH_3)_3$[c]	-410.91210	119.9	0
	$N(CH_3)_3$[d]	-410.91209		

a) Py = pyrrole
b) An entry of 0 means that there are no imaginary frequencies; frequencies in cm^{-1}.
c) Proton acceptor with one H or one C in the plane of the pyrrole
d) Proton acceptor with one H or one C in the plane perpendicular to the plane of the pyrrole
e) Rotation of proton acceptor
f) Ring puckering of the substituted pyrrole out of the plane of pyrrole ring

frequency in some of these complexes corresponds to rotation of the proton acceptor molecule about the hydrogen-bonding axis. However, the energies of the two rotamers, one with an H of NH_3 or a C of $N(CH_3)_3$ in the plane of the pyrrole ring, and the other with an H of NH_3 or a C of $N(CH_3)_3$ in the plane perpendicular to the plane of the pyrrole ring, are identical, as evident from Table 4. This indicates that there is free rotation of the proton acceptor molecule about the hydrogen bonding N-N axis. The complexes with the N-H or N-C bonds in the plane of the pyrrole ring will be discussed below. The complex 2,5-diberylliumpyrrole:$N(CH_3)_3^{+2}$ has two imaginary frequencies. The frequency of –12 cm^{-1} corresponds to rotation of $N(CH_3)_3$ about the hydrogen-bonding axis. The frequency of -40 cm^{-1} corresponds to a ring puckering vibration. However, since these frequencies are small, this complex has been included in this study. The energies in Tables 1-4 are given as raw data from which binding energies and enthalpies can be computed. The z-matrices for the optimized monomers and complexes are given in Appendix 1 and 2, respectively. The binding enthalpies for the complexes are reported in Appendix 3.

Table 5 reports equilibrium N_a-N_b distances [$R_e(N_a\text{-}N_b)$], N_a-H distances [$R_e(N_a\text{-}H)$], electronic binding energies (ΔE_e), harmonic proton-stretching frequencies (υ) and intensities of the proton-stretching band (I) for complexes of pyrrole and disubstituted pyrroles with HCN and its derivatives. The complexes are arranged in order of increasing acidity of pyrrole and disubstituted pyrroles as determined by their binding energy with HCN. For a given proton donor, the complexes are arranged in order of increasing base strength as determined by the electronic proton affinity of the proton acceptor.

Table 5. MP2/6-31+G(d,p) N_a-N_b and N_a-H distances (R_e, Å), electronic binding energies (ΔE_e, kcal/mol), harmonic proton-stretching frequencies (υ, cm^{-1}) and band intensities (I, km/mol) for complexes of pyrrole and substituted pyrroles with HCN and its derivatives.

Donor[a]	Acceptor	$R_e(N_a\text{-}N_b)$	$R_e(N_a\text{-}H)$[b]	ΔE_e	ν	I
Py	HCN	3.164	1.011	- 5.3	3671	466
	LiCN	3.010	1.019	-10.1	3527	989
	NaCN	2.971	1.021	-11.6	3483	1171
	SCN^{-1}	2.835	1.037	-18.5	3198	2653
	OCN^{-1}	2.762	1.048	-22.5	2993	2761
3,4-diFPy	HCN	3.115	1.012	- 6.4	3656	591
	LiCN	2.956	1.022	-12.6	3472	1249
	NaCN	2.916	1.025	-14.4	3414	1477
	SCN^{-1}	2.770	1.045	-24.1	3034	3388
	OCN^{-1}	2.699	1.061	-28.9	2767	3442
2,5-diFPy	HCN	3.068	1.016	- 6.6	3594	777
	LiCN	2.906	1.029	-12.4	3343	1662
	NaCN	2.863	1.033	-14.3	3260	2023
	SCN^{-1}	2.713	1.065	-21.8	2710	4750
	OCN^{-1}	2.629	1.097	-26.9	2202	6340
3,4-diBePy^{+2}	HCN	2.828	1.043	-21.0	3127	2706
	LiCN	2.603	1.119	-46.5	1924	6469
	NaCN[c]	2.666	1.557	-54.6	1871	2836
					2473	4208

a) Py = pyrrole

b) The N_a-H distance is measured from the pyrrole nitrogen.

c) There are two strong bands associated with the N_a-H stretching mode in this complex.

The first set of complexes in Table 5 are those with pyrrole as the proton donor. Table 5 shows that for these complexes as the base strength increases, the binding energy increases. The binding energies range from –5.3 kcal/mol for the weakest hydrogen-bonded complex pyrrole:NCH, to –22.5 kcal/mol for the strongest, pyrrole:NCO^-. As evident from Table 5, as the binding energy increases the N_a-H distance also increases from 1.011 Å in pyrrole:NCH to 1.048 Å in pyrrole:NCO^-. These N_a-H bond distances are all greater than the N_a-H distance in isolated pyrrole (1.007 Å). The lengthening of the N_a-H bond is a consequence of hydrogen bonding. Moreover, the lengthening of the N_a-H distance is also accompanied by a decrease in the N_a-N_b distance, which ranges from 3.164 Å in pyrrole:NCH to 2.762 Å in pyrrole:NCO^-. Figure 2 illustrates the variation of the N_a-H and N_a-N_b distances with binding energy. These data show that as the binding energy increases, the hydrogen moves away from N_a towards N_b. This is the beginning of proton transfer, which is facilitated by a decrease in the N_a-N_b distance.

The IR properties of the complexes of pyrrole with HCN and its derivatives may also be related to their structural and energetic properties. As the base strength increases, the proton-stretching frequency decreases, and the intensity of the proton-stretching band increases. The proton-stretching frequency and the intensity of the proton-stretching band for isolated pyrrole are 3735 cm^{-1} and 80 km/mol, respectively. The proton-stretching frequency decreases from 3671 cm^{-1} in pyrrole:NCH to 2993 cm^{-1} in pyrrole:NCO^-. At the same time, the intensity of the proton-stretching band increases from 466 km/mol in pyrrole:NCH to 2761 km/mol in pyrrole:NCO^-. The frequency

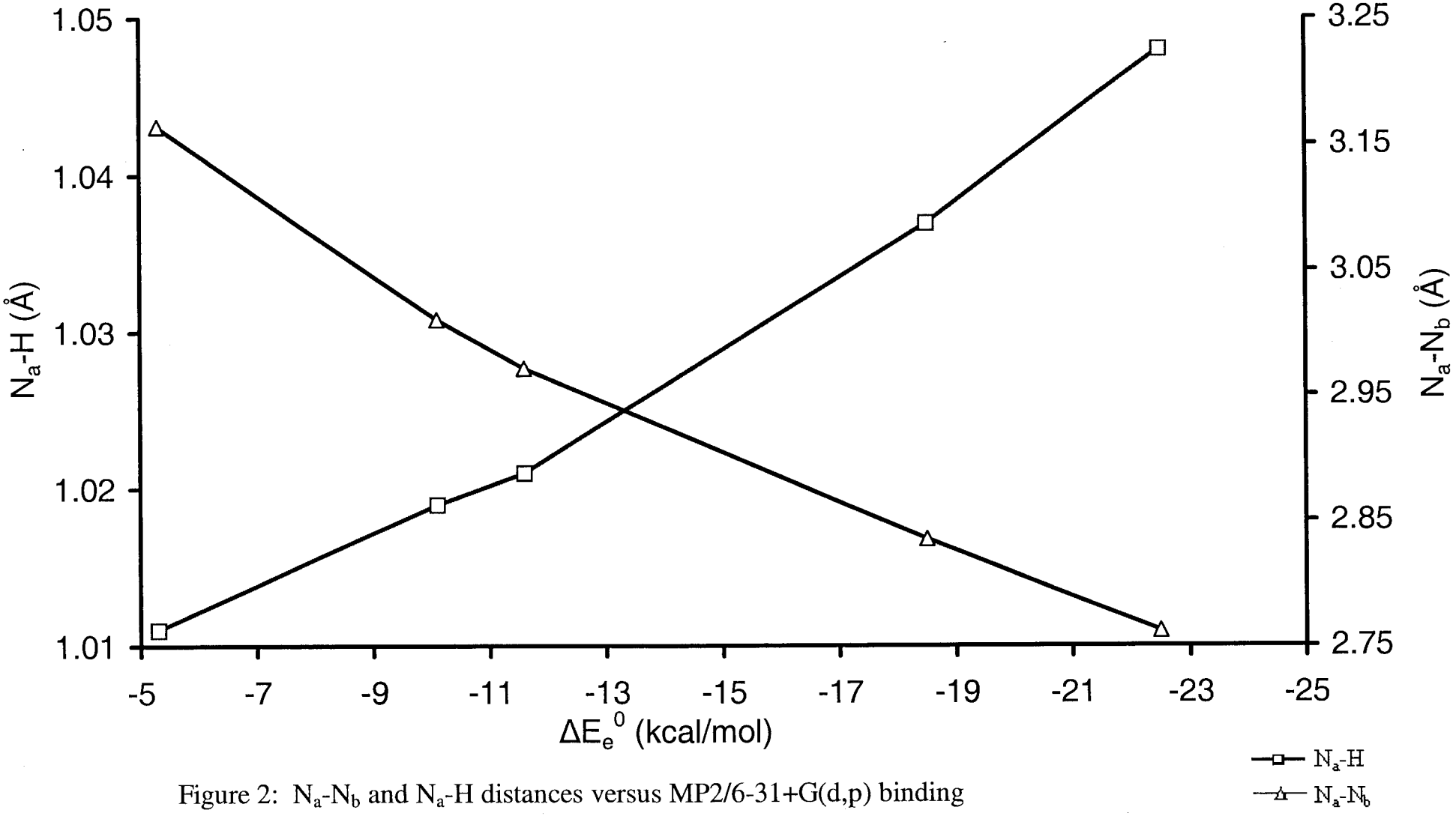

Figure 2: N_a-N_b and N_a-H distances versus MP2/6-31+G(d,p) binding energies of complexes with pyrrole as the proton donor to HCN and its derivatives

shifts and the increased intensities of the proton-stretching band in the complexes relative to pyrrole are typical of hydrogen-bonded complexes, and are the IR signature of the hydrogen bond.

The variation in the frequency and intensity of the proton-stretching band for the complexes with pyrrole as the proton donor is illustrated in Figure 3. The vibrational spectra are arranged in order of increasing base strength. The intensity of the proton-stretching band is much greater compared to the other fundamental bands, which cannot be seen on the scale shown in Figure 3. For the charged complexes of pyrrole:NCS^- and pyrrole:NCO^-, one additional relatively intense band at 2015 cm^{-1} and at 2206 cm^{-1}, respectively, can be seen. These correspond to monomer NCO^- and NCS^- stretching vibrational modes that are essentially unchanged in the complexes. The spectra in figure 3 illustrate that as the N_a-H distance increases, the N_a-H bond becomes weaker. This implies a decrease of the force constant for the N_a-H stretch, which leads to a decrease in the proton-stretching frequency. In addition, as the proton moves towards the base, the dipole moment of the complex increases. As a result, the intensity of the proton-stretching band also increases.

The data in Table 5 indicate that complexes with pyrrole as the proton donor to HCN and its derivatives are stabilized by traditional hydrogen bonds.[42] In these complexes the N_a-H covalent bond remains intact, and the N_a-N_b distances are typical of complexes stabilized by traditional hydrogen bonds.[42] The spectra of these hydrogen-bonded complexes are characterized by a single intense proton-stretching band that is shifted to lower energy relative to the monomer stretching frequency.

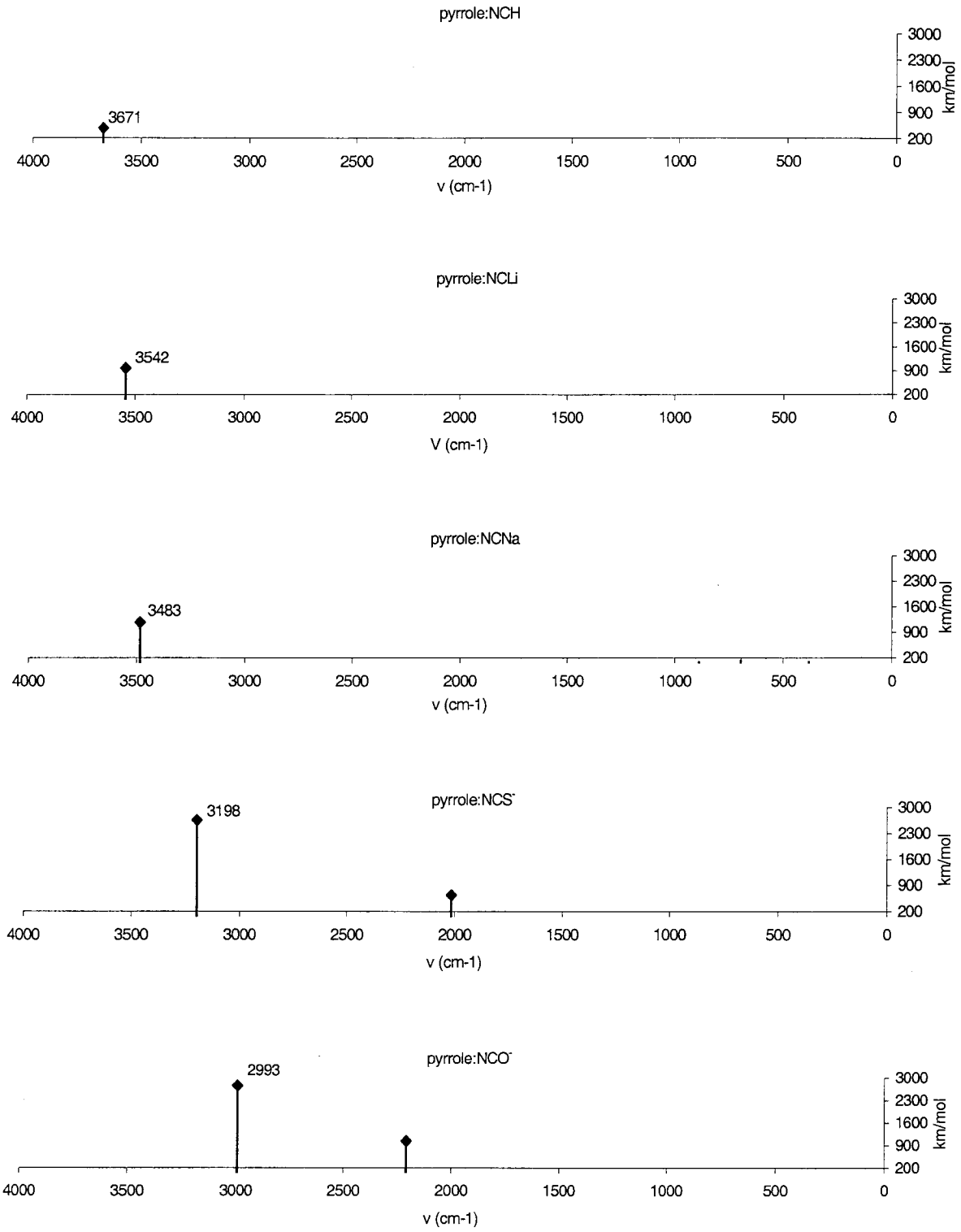

Figure 3: MP2/6-31+G(d,p) vibrational spectra of pyrrole:NCH, pyrrole:NCLi, pyrrole:NCNa, pyrrole:NCS^- and pyrrole:NCO^-. Only bands with intensities greater than 250 km/mol are shown.

The next set of complexes in Table 5 are those with 3,4-difluoropyrrole as the proton donor to HCN and its derivatives. For this set of complexes, it is again seen that as the base strength increases the binding energy increases. The binding energies range from –6.4 kcal/mol or 3,4-difluoropyrrole:NCH to –28.9 kcal/mol for 3,4-difluoropyrrole:NCO^-. As the binding energy increases, the N_a-H distance increases from 1.012 Å in 3,4-difluoropyrrole:NCH to 1.061 Å in 3,4-difluoropyrrole:NCO^-. Moreover, as the N_a-H distance increases the N_a-N_b distance decreases from 3.115 Å for 3,4-difluoropyrrole:NCH to 2.699 Å for 3,4-difluoropyrrole:NCO^-. Thus, the same trends in binding energies, as well as N_a-H and N_a-N_b distances, seen previously in the complexes with pyrrole, are observed in complexes with 3,4-difluoropyrrole.

The IR properties of the complexes of 3,4-difluoropyrrole with HCN and its derivatives are also related to the structural and energetic properties. As the base strength increases, the proton-stretching frequency decreases, and the intensity of the proton-stretching band increases. The 3,4-difluoropyrrole monomer has an N_a-H stretching frequency of 3745 cm^{-1}, and the band intensity is 110 km/mol. In the complexes, the proton-stretching frequency decreases from 3656 cm^{-1} in 3,4-difluoropyrrole:NCH to 2767 cm^{-1} in 3,4-difluoropyrrole:NCO^-. The intensity of the proton-stretching band increases from 591 km/mol in 3,4-difluoropyrrole:NCH to 3442 km/mol in 3,4-difluoropyrrole:NCO^-. The frequency shifts and increased intensities of the proton-stretching band in the complexes relative to the monomer are due to hydrogen bonding.

The complexes with 3,4-difluoropyrrole as the proton donor with HCN and its derivatives are also stabilized by traditional hydrogen bonds. The N_a-H distances in these complexes are characteristic of a perturbed covalent N_a-H bond, and the N_a-N_b distances

are typical of traditional hydrogen bonds.[42] Furthermore, the vibrational spectra of these complexes are characterized by a single proton-stretching band which is shifted to lower energy relative to 3,4-difluoropyrrole.

Data for complexes of 2,5-difluoropyrrole with HCN and its derivatives are also reported in Table 5. Once again as the base strength increases, the binding energy increases, the N_a-H distance increases, and the N_a-N_b distance decreases. The binding energies vary from –6.6 kcal/mol for 2,5-difluoropyrrole:NCH to –26.9 kcal/mol for 2,5-difluoropyrrole:NCO^-. The N_a-H distances increases from 1.016 Å for 2,5-difluoropyrrole:NCH to 1.097 Å for 2,5-difluoropyrrole:NCO^-. The N_a-N_b distance decreases from 3.068 Å for 2,5-difluoropyrrole:NCH to 2.629 Å for 2,5-difluoropyrrole:NCO^-. Thus, the same trends in binding energies and N_a-H and N_a-N_b distances for complexes of pyrrole and 3,4-difluoropyrrole are observed for the complexes with 2,5-difluoropyrrole.

The IR properties of the complexes of 2,5-difuoropyrrole with HCN and its derivatives are again related to the structural and energetic properties. As the binding energy increases, the proton-stretching frequency decreases, and the intensity of the proton-stretching band increases. The proton-stretching frequency and the intensity of the proton-stretching band for 2,5-difluoropyrrole are 3730 cm^{-1} and 149 km/mol, respectively. The proton-stretching frequency decreases from 3594 cm^{-1} for 2,5-difluoropyrrole:NCH to 2202 cm^{-1} for 2,5-difluoropyrrole:NCO^-. The intensity of the proton-stretching band increases from 777 km/mol for 2,5-difluoropyrrole:NCH to 6340 km/mol for 2,5-difluoropyrrole:NCO^-.

All the complexes of 2,5-difluoropyrrole as the proton donor to HCN and its derivatives, except 2,5-difluoropyrrole:NCO^-, are stabilized by traditional hydrogen bonds. The N_a-H distances and N_a-N_b distances of these complexes are typical of traditional hydrogen bonds,[42] and their vibrational spectra are characterized by a single intense proton-stretching band that is shifted to lower energy relative to the N_a-H stretch of the 3,4-difluoropyrrole monomer.

The complex 2,5-difluoropyrrole:NCO^- has an N_a-H distance of 1.097 Å, and a very short N_a-N_b distance of 2.629 Å. These distances are approaching distances found for proton-shared N-H-N hydrogen bonds.[42] The N_a-H distance of this complex cannot be simply described as a perturbed N_a-H distance. Furthermore, the proton-stretching band has dramatically shifted to lower energy by 1528 cm^{-1} relative to the 2,5-difluoropyrrole monomer. This spectral property also indicates that the hydrogen bond in 2,5-difluoropyrrole:NCO^- has proton-shared character. Thus, a hydrogen bond with proton-shared character is found in this negatively charged complex.

Only three complexes with 3,4-diberylliumpyrrole^{+2} as the proton donor are listed in Table 5. The first is 3,4-diberylliumpyrrole:NCH^{+2}, which has a binding energy of -21.0 kcal/mol. The N_a-H and N_a-N_b distances for this complex are 1.043 Å and 2.828 Å, respectively, which are comparable to distance seen in complexes with traditional hydrogen bonds. Furthermore, the vibrational spectrum of this complex is characterized by a single intense proton-stretching band at 3127 cm^{-1} with a band intensity of 2706 km/mol. These data are typical for a complex stabilized by a traditional hydrogen bond.

The structural, energetic and spectroscopic properties of the complex 3,4-diberylliumpyrrole:$NCLi^{+2}$ are different. The binding energy for this complex has

dramatically increased to –46.5 kcal/mol. Furthermore, the N_a-H distance has increased to 1.119 Å, and the N_a-N_b distance has decreased to 2.603 Å. Thus, this complex has the longest N_a-H distance and shortest N_a-N_b distance observed so far, and is stabilized by a proton-shared hydrogen bond. For the complex of 3,4-diberylliumpyrrole:$NCLi^{+2}$ the proton-stretching frequency has decreased to 1924 cm^{-1} and the intensity of the proton-stretching band has increased to 6469 km/mol. This frequency is the lowest thus far, and corresponds to a shift of 1696 cm^{-1} relative to 3,4-diberylliumpyrrole^{+2}. Thus, both structural and spectral data for this cationic complex lead to the characterization of the hydrogen bond as a proton-shared hydrogen bond.

The last complex in Table 5 is 3,4-diberylliumpyrrole:$NCNa^{+2}$. The binding energy of this complex is –54.6 kcal/mol, the largest in Table 5. The N_a-H distance for this complex has dramatically increased to 1.557 Å, and the N_a-N_b distance has increased to 2.666 Å relative to 3,4-diberylliumpyrrole:$NCLi^{+2}$. Thus, the N_b-H distance is 1.109 Å, indicating a perturbed covalent N_b-H^+ bond. Therefore, the hydrogen bond in this complex is on the ion-pair side of proton-shared. That is, if 3,4-diberylliumpyrrole:$NCLi^{+2}$ and 2,5-difluoropyrrole:NCO^- have proton-shared hydrogen bonds, then 3,4-diberylliumpyrrole:$NCNa^{+2}$ must have a hydrogen bond with ion-pair character. This is also supported by the spectrum of this complex, which is characterized by two strong proton-stretching bands appearing at 1871 and 2473 cm^{-1}, with intensities of 2836 and 4208 km/mol, respectively. The strongest band at 2473 cm^{-1} is at a higher frequency compared to 3,4-diberylliumpyrrole:$NCLi^{+2}$, further indicating the ion-pair character of this complex. The proton-stretching band is due to a perturbed N_b-H stretch, shifted to lower frequency relative to $HNCNa^{+1}$. The fact that there are two bands in the

spectrum is due to coupling of the N_b-H stretch to the N-C stretch of $HCNNa^{+1}$. The local N-C stretching band increases in intensity due to intensity borrowing from the N_b-H stretch.

Complexes of pyrrole and disubstituted pyrroles with NH_3 and trimethylamine have C_s symmetry, and binding energies, N_a-N_b and N_a-H distances, proton-stretching frequencies, and intensities of the proton-stretching bands are reported in Table 6. These complexes are arranged in order of increasing N_a-H distance so that changes in hydrogen bond type can be observed.

The first seven complexes listed in Table 6, namely, pyrrole:NH_3, 3,4-difluoropyrrole:NH_3, pyrrole:$N(CH_3)_3$, 2,5-difluoropyrrole:NH_3, 3,4-difluoropyrrole:$N(CH_3)_3$, 2,5-diberylliumpyrrole:NH_3^{+2} and 2,5-difluoropyrrole:$N(CH_3)_3$ are stabilized by traditional hydrogen bonds. The N_a-H distances for these complexes increase from 1.021 Å for pyrrole:NH_3 to 1.053 Å for 2,5-difluoropyrrole:$N(CH_3)_3$, while the N_a-N_b distances decrease from 3.034 Å for pyrrole:NH_3 to 2.785 Å for 2,5-difluoropyrrole:$N(CH_3)_3$. These distances correspond to N_a-H and N_a-N_b distances already seen in Table 5 for complexes with traditional hydrogen bonds. The proton-stretching frequencies for these complexes decrease from 3484 cm^{-1} for pyrrole:NH_3 to 2848 cm^{-1} for 2,5-difluoropyrrole:$N(CH_3)_3$, and the intensities of the proton-stretching bands increase from 862 km/mol for pyrrole:NH_3 to 3237 km/mol for 2,5-difluoropyrrole:$N(CH_3)_3$. The vibrational spectra are characterized by a single strong proton-stretching band consistent with the spectra of complexes with traditional hydrogen bonds seen in Table 5. It is expected that the binding energies for these complexes should increase from pyrrole:NH_3 to 2,5-difluoropyrrole:$N(CH_3)_3$. However, this trend is

Table 6. MP2/6-31+G(d,p) N_a-N_b and N_a-H distances (R_e, Å), electronic binding energies(ΔE_e, kcal/mol), harmonic proton-stretching frequencies (ν, cm^{-1}) and band intensities (I, km/mol) for complexes of pyrrole and substituted pyrroles with NH_3 and $N(CH_3)_3$

Donor[a]	Acceptor	R_e(N-N)	$R_e(N_a\text{-H})$[b]	ΔE_e	ν	I
Py	NH_3	3.034	1.021	- 8.6	3484	862
3,4-diFPy	NH_3	2.992	1.023	-10.1	3429	1086
Py	$N(CH_3)_3$	2.931	1.029	-10.1	3305	1453
2,5-diFPy	NH_3	2.924	1.032	-11.3	3272	1560
3,4-diFPy	$N(CH_3)_3$	2.881	1.035	-11.8	3196	1773
2,5-diBePy^{+2}	NH_3	2.870	1.050	-23.0[c]	2964	1857
2,5-diFPy	$N(CH_3)_3$	2.785	1.053	-13.9	2848	3237
3,4-diBePy^{+2}	NH_3	2.698	1.107	-26.2	2071	5305
2,5-diBePy^{+2}	$N(CH_3)_3$	2.837	1.773	-33.1[c]	2772	1972
3,4-diBePy^{+2}	$N(CH_3)_3$	2.875	1.822	-46.0	2961	2264

a) Py = pyrrole

b) The N_a-H distance is measured from the pyrrole nitrogen.

c) Strong electrostatic interactions of Be^+ with the nitrogen of the proton acceptor contribute to the large stabilization energy of this complex

only observed if 2,5-diberylliumpyrrole:NH_3 is excluded. The binding energy for the complex 2,5-diberylliumpyrrole:NH_3^{+2} is –23.0 kcal/mol and is greater than the binding energy of the complex immediately below it in Table 6. The increased stabilization is due to strong electrostatic interactions of the Be^+ atoms with the nitrogen of the proton acceptor.

The next complex in Table 6 is 3,4-diberylliumpyrrole:NH_3^{+2}. This complex is stabilized by a proton-shared hydrogen bond and has a binding energy of –26.2 kcal/mol. In this complex, the N_a-N_b distance has decreased to 2.698 Å, and the N_a-H distance has increased to 1.107 Å. Furthermore, the proton-stretching frequency of this complex is 2071 cm^{-1} and the intensity of the proton-stretching band is 5305 km/mol. The shift relative to 3,4-diberylliumpyrrole^{+2} is 1549 cm^{-1}. The N_a-H and N_a–N_b distances and proton stretching frequency are similar to those observed for complexes with proton-shared hydrogen bonds in Table 5. Therefore, this cationic complex is stabilized by a proton-shared hydrogen bond.

The last two complexes in Table 6, 2,5-diberylliumpyrrole:$N(CH_3)_3^{+2}$ and 3,4-diberylliumpyrrole:$N(CH_3)_3^{+2}$, are stabilized by ion-pair hydrogen bonds. For these two complexes the N_a-N_b distances have increased relative to 3,4-diberylliumpyrrole:NH_3^{+2} to 2.837 Å and 2.875 Å. The N_a-H distances are very long at 1.773 Å and 1.822 Å, respectively. Thus, the N_b-H^+ distances are 1.064 Å in 2,5-diberylliumpyrrole:$N(CH_3)_3^{+2}$ and 1.053 Å in 3,4-diberylliumpyrrole:$N(CH_3)_3^{+2}$. Thus, the N_b-H^+ bond is a perturbed N_b-H^+ bond of protonated trimethylamine. The N_b-H distance in isolated $HN(CH_3)_3^{+1}$ is 1.024 Å. Furthermore, the IR spectra of these complexes are characterized by a single strong proton-stretching band at 2772 cm^{-1} for 2,5-diberylliumpyrrole:$N(CH_3)_3^{+2}$ and

2961 cm^{-1} for 3,4-diberylliumpyrrole:$N(CH_3)_3^{+2}$, with band intensities of 1972 km/mol and 2264 km/mol, respectively. These proton-stretching bands are best described as arising from perturbed N_b-H^+ stretches. These bands are shifted to lower frequency compared to the proton-stretching frequency of 3501 cm^{-1} for $HN(CH_3)_3^{+1}$. Therefore, the structural and spectroscopic data for these two complexes indicate that they are stabilized by ion-pair hydrogen bonds. The binding energies for these complexes are -33.1 kcal/mol for 2,5-diberylliumpyrrole:$N(CH_3)_3^{+2}$ and –46.0 kcal/mol for 3,4-diberylliumpyrrole:$N(CH_3)_3^{+2}$. Thus, ion-pair hydrogen-bonded complexes occur when the strongest cationic proton donors, 3,4-diberylliumpyrrole^{+2} and 2,5-diberylliumpyrrole^{+2} are combined with the strong proton acceptor, $N(CH_3)_3$.

The characteristic changes in the N_a-N_b and N_a-H distances and proton-stretching frequencies that accompany changes in hydrogen bond type are illustrated in Figure 4. In this figure, the N_a-N_b distance and the proton-stretching frequency are plotted against the N_a-H distance for the series of complexes of pyrrole and disubstituted pyrroles with ammonia and trimethylamine. At short N_a-H distances, traditional hydrogen bonds are found, and the N_a-N_b distance and the proton-stretching frequency change almost linearly with the N_a-H distance. The points in this region of the graph correspond to the first seven complexes in Table 6, which are stabilized by traditional hydrogen bonds. Figure 4 suggests that the change from a traditional to a proton-shared hydrogen bond is not a dramatic one. Nevertheless, the two points which correspond to the shortest N_a-N_b distance and lowest proton-stretching frequency, are found for the complex with a proton-shared hydrogen bond. Subsequently, there is a rather dramatic change in the

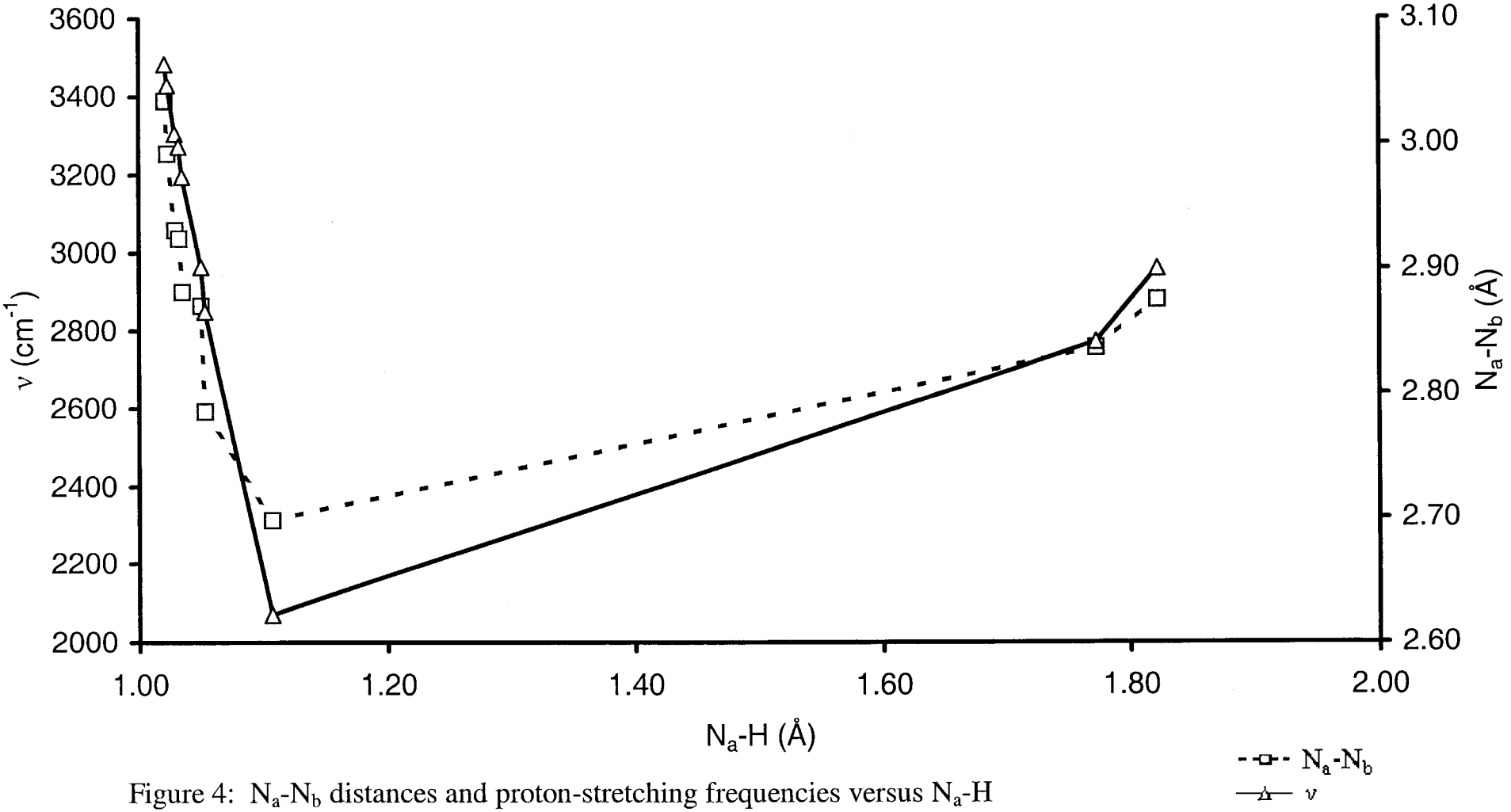

Figure 4: N_a-N_b distances and proton-stretching frequencies versus N_a-H distances in complexes of pyrrole and disubstituted pyrroles with NH_3 and $N(CH_3)_3$

slope of the two lines which signals the formation of ion-pair hydrogen bonds. It would be interesting to have had at least one more point for a complex in this series in which the N_a-H distance had a value of about 1.2 Å. Such a point would indicate whether proton-shared hydrogen bonds span a relatively narrow range of N_a-H distances or not. Unfortunately, no such point exists for the complexes investigated in this work.

IV. CONCLUSIONS:

Optimized MP2/6-31+G(d,p) structures have been determined for the complexes of pyrrole and disubstituted pyrroles with the nitrogen bases HCN, LiCN, NaCN, SCN^-, OCN^-, NH_3 and $N(CH_3)_3$. The harmonic vibrational spectra of these complexes have also been calculated at MP2/6-31+G(d,p). The following statements are supported by these calculations.

1. By systematically varying the proton-donating ability of pyrrole and substituted pyrroles and the proton-accepting ability of nitrogen bases, complexes stabilized by traditional N-H...N, proton-shared N...H...N, and ion-pair $N^-...{}^+H$-N hydrogen bonds have been produced.
2. Proton-shared and ion-pair hydrogen bonds are not found in neutral complexes. They occur only in charged complexes.
3. Most of the complexes investigated in this study are stabilized by traditional hydrogen bonds as evident from the N_a-H distances, N_a-N_b distances, and proton-stretching frequencies. In series of closely related complexes stabilized by traditional hydrogen bonds, as the base strength increases, the binding energy increases, the N_a-N_b distance

decreases, the N_a-H distance increases, the proton-stretching frequency decreases, and the intensity of the proton-stretching band increases.

4. Among the complexes with HCN and its derivatives as proton acceptors, two charged complexes are stabilized by proton-shared hydrogen bonds, and a third is stabilized by a hydrogen bond which is on the ion-pair side of proton-shared. Proton-shared hydrogen bonds have short intermolecular N_a-N_b distances, long N_a-H and N_b-H distances, and proton-stretching frequencies that are dramatically shifted to lower energy compared to traditional and ion-pair hydrogen bonds.
5. Among complexes with NH_3 as the proton acceptor, only traditional hydrogen bonds are formed. When the stronger base $N(CH_3)_3$ is the proton acceptor, one charged complex has a proton-shared hydrogen bond, and two charged complexes have ion-pair hydrogen bonds.
6. This study suggests that proton-shared and ion-pair hydrogen bonds probably do not exist in neutral complexes stabilized by N-H-N hydrogen bonds.

V. REFERENCES:

1. Hanessian, S.; Yang , H.; Schaum, R. *J. Am. Chem. Soc.* **1996**, *118*, 2507.
2. Cantor, C. R., Schimmel, P. P. *Biophysical Chemistry*; Freeman: San Francisco, CA, **1980**; Vol 1.
3. Baker, E. N.; Hubbard, R. E. *Prog. Biophys. Mol. Biol.* **1984**, *44*, 97.
4. Schramm, V. L.; Purich, D. L. *Methods in Enzymology*; Academic Press: San Diego, CA, **1999**; Vol. 308, pp 219-297.
5. Del Bene, J. E.; Person, W. B.; Szczepaniak, K. *Chem. Phys. Lett.* **1995**, *247*, 89.
6. Del Bene, J. E.; Person, W. B.; Szczepaniak, K. *Mol. Phys.* **1996**, *89*, 47.
7. Del Bene, J. E.; Jordan, M. J. T. *Int. Rev. Phys. Chem.* **1999**, *18*, 119.
8. Morokuma, K.; Pedersen, L. *J. Chem Phys.* **1968**, *49*, 3275.
9. Kollman, P. A.; Allen, L. C. *J. Chem Phys.* **1969**, *51*, 3286.
10. Morokuma, K.; Winick, J. *J. Chem Phys.* **1970**, *52*, 1301.
11. Del Bene, J.; Pople, J. A. *J. Chem Phys.* **1970**, *52*, 4858.
12. Hankins, D.; Moskowitz, J. W.; Stillinger, F. H. *Chem. Phys. Lett.* **1970**, *4*, 527.
13. Pople, J. A.; Krishnan, R.; Schlegel, H. B.; Binkley, J. S. *Int. J. Quantum Chem.* **1979**, *13S*, 225.
14. Schlegel, H. B., *J. Comput. Chem.* **1982**, *3*, 214.
15. Schlegel, H. B.; Brinkely, J. S.; Pople, J. A. *J. Chem. Phys.* **1984**, *80*, 1979.
16. Fogarasi, G.; Pulay, P. *Ann. Rev. phys. Chem.* **1984**, *35*, 191.
17. Pulay, P. *Adv. Chem. Phys.* **1987**, *69*, 241.

18. Dykstra, C. E.; Augspurger, J. D.; Kirtman, B.; Malik, D. J. *Reviews of Computational Chemistry*, Lipkowitz, K. B.; Boyd, D. B., Eds.; VCH: NY, **1990**; Vol. 1, pp 83-118.

19. Bartlett, R. J.; Stanton, J. F.; Watts, J. D. *Reviews of Computational Chemistry*, Lipkowitz, K. B.; Boyd, D. B., Eds.; VCH: NY, **1991**; Vol V., pp 65-169.

20. Gauss, J.; Cremer, D. *Adv. Quant. Chem.* **1992**, *23*, 206.

21. Pimentel, G. C.; McClellan, A. L. *The Hydrogen Bond,* Freeman: San Francisco, CA, **1960**.

22. Del Bene, J. E. Hydrogen Bonding:1. *Encyclopedia of Computational Chemistry*; Schyleyer, P. v.; Allinger, N. L.; Clark, T.; Gasteiger, J.; Kollman, P. A.; Schaefer, H. F. , III; Schreiner, P. R., Eds.; Wiley & son: Chichester, UK, **1998**; Vol. 2, pp 1263-1271.

23. Beckenham, K. Hydrogen Bonding and Other Physicochemical Interactions Studied By IR and Raman Spectroscopy. *Encyclopedia of Spectroscopy and Spectrometry*, London, J. C.; Tranter, G. E.; Holmes, J. L., Eds.; Academic Press: UK, **1999**, Vol. 1, pp 837-843.

24. Scheiner, S. *Hydrogen Bonding: A Theoretical Perspective*, Oxford University Press: NY, **1997**.

25. Scheiner, S. Calculating the Properties of Hydrogen Bonds by ab Initio Methods. *Reviews of Computational Chemistry*, Lipkowitz, K. B.; Boyd, D. B., Eds.; VCH: NY, **1991**, Vol 2, pp 165-264.

26. Del Bene, J. E.; Jordan, M. J. T. *J. Chem. Phys.* **1998**, *108*, 3205.

27. Del Bene, J. E.; Jordan, M. J. T. *J. Am. Chem. Soc.* **2000**, *122*, 2101.

28. Tai, J. C.; Yang, L.; Allinger N. L. *J. Am. Chem. Soc.* **1993**, *115*, 11906.

29. Lee, S. Y.; Boo, B. H. *J. Phys. Chem.* **1996**, *100*, 15073.

30. Jiang, J. C.; Tsai M. H. *J. Phys. Chem.* **1997**, *101*, 1982.

31. Hehre W. J.;Radom, L.; Schleyer, P. v.R.; Pople, J. A. *Ab initio Molecular Orbital Theory*; John Wiley & Son: Toronto, Canada, **1986**.

32. Bartlett, R. J.; Stanton, J. F. Applications of Post-Hartree-Fock Methods: A Tutorial. *Reviews of Computational Chemistry,* Lipkowitz, K. B.; Boyd, D. B., Eds.; VCH: NY, **1994**, Vol. V, pp 65-169.

33. Pople, J. A.; Beveridge, D. L. *Approximate Molecular Orbital Theory*; McGraw Hill Book Company: NY, **1970**.

34. Atkins, P. W.; Friedman, R. S. *Molecular Quantum Mechanics*, 3rd edition; Oxford University Press: NY, **1997**.

35. Del Bene, J. E. *J. Comput. Chem.* **1987**, *8*, 810.

36. Del Bene, J. E. *J. Chem. Phys.* **1987**, *86*, 2110.

37. Del Bene, J. E. *International Journal of Quantum Chemistry: Quantum Biology Symposium* **1987**, *14*, 27.

38. Del Bene, J. E. *J. Phys. Chem.* **1988**, *92*, 2874.

39. Del Bene, J. E.; Shavitt, I. *J. Mol. Struct.* **1994**, 307, 27.

40. Tzeli, D.; Mavridis, A.; Xantheas, S. S. *J. Chem. Phys.* **2000**, 112, 6178.

41. Frisch, M. J.; Trucks, G. W.; Schlegel, H. B.; Scuseria, G. E.; Robb, M. A.; Cheeseman, J. R.; Zakrzewski, V. G.; Montgomery, J. A.; Stratmann, R. E. Jr.; Burant, J. C.; Dapprich, S.; Millam, J. M.; Daniels, A. D.; Kudin, K. N.; Strain, M. C.; Farkas, O.; Tomasi, J.; Barone, V.; Cossi, M.; Cammi, R.; Mennucci, B.;

Pomelli, C.; Adamo, C.; Clifford, S.; Ochterski, J.; Petersson, G. A.; Ayala, P. Y.; Cui, Q.; Morokuma, K.; Malick, D. K.; Rabuck, A. D.; Raghavachari, K.; Foresman, J. B.; Cioslowski, J.; Ortiz, J. V.; Baboul, A. G.; Stefanov, B. B.; Liu, G.; Liashenko, A.; Piskorz, P.; Komaromi, I.; Gomperts, R.; Martin, R. L.; Fox, D. J.; Keith, T.; Al-Laham, M. A.; Peng, C. Y.; Nanayakkara, A.; Gonzalez, C.; Challacombe, M.; Gill, P. M. W.; Johnson, B.; Chen, W.; Wong, M. W.; Andres, J. L.; Gonzalez, C.; Head-Gordon, M.; Replogle, E. S.; Pople, J. A. *Gaussian 98*; Gaussian, Inc.: Pittsburgh, PA, **1998**.

42. Del Bene, J. E.; Perera, A.; Bartlett, R. J. *J. Phys. Chem. A.* **2000**, 105, 930.

Appendix 1

Z-matrices for optimized monomers reported in Tables 1 and 2, taken directly from Gaussian 98 output

---
HCN MP2/6-31+G(D,P) OPTIMIZED STRUCTURE

Symbolic Z-matrix:
Charge = 0 Multiplicity = 1

```
C
N    1    CN
X    1    1.      2    90.
H    1    CH      3    90.      2    180.      0
```

Variables:

CH	1.06652
CN	1.17845

LICN MP2/6-31+G(D,P) OPTIMIZED STRUCTURE

Symbolic Z-matrix:
Charge = 0 Multiplicity = 1
C
N 1 CN
X 1 1. 2 90.
Li 1 CLI 3 90. 2 180. 0

Variables:
CN 1.19257
CLI 1.94586

NCNa MP2/6-31+G(D,P) OPTIMIZED STRUCTURE WITH ONLY THE 1s ORBITALS FROZEN

Symbolic Z-matrix:
Charge = 0 Multiplicity = 1

```
X
N    1    1.
C    2    CN       1    90.
X    3    1.       2    90.      1    0.       0
Na   3    CNa      4    90.      1    180.     0
```

Variables:

CN	1.192947
CNa	2.228593

NCS$^-$ MP2/6-31+G(D,P) OPTIMIZED STRUCTURE

Symbolic Z-matrix:

Charge =-1 Multiplicity = 1

```
X
N    1    1.
C    2    CN      1    90.
X    3    1.      2    90.      1    0.       0
S    3    CS      4    90.      1    180.     0

   Variables:
CN                1.2022
CS                1.66173
```

NCO$^-$ MP2/6-31+G(D,P) OPTIMIZED STRUCTURE

Symbolic Z-matrix:

Charge =-1 Multiplicity = 1

```
N
C    1    CN
X    2    1.      1    90.
O    2    CO      3    90.      1    180.      0
```

Variables:

CN	1.21407
CO	1.24452

NH_3 MP2/6-31+G(D,P) OPTIMIZED STRUCTURE

Symbolic Z-matrix:
Charge = 0 Multiplicity = 1

N							
X	1	1.					
H	1	R	2	A			
H	1	R	2	A	3	120.	0
H	1	R	2	A	3	-120.	0

Variables:

R	1.0117
A	110.82744

$N(CH_3)_3$ MP2/6-31+G(D,P) OPTIMIZED STRUCTURE

Symbolic Z-matrix:

Charge = 0 Multiplicity = 1

```
X
N   1   1.
X   1   1.      2   90.
X   1   1.      3   90.     2   0.      0
C   2   CN      1   ANG      3   0.      0
H   5   CH6     2   ANG6     1   180.    0
H   5   CH7     2   ANG7     6   120.    0
H   5   CH7     2   ANG7     6   -120.   0
X   2   1.      1   90.      3   120.    0
C   2   CN      1   ANG      3   120.    0
H   10  CH6     2   ANG6     9   180.    0
H   10  CH7     2   ANG7     11  120.    0
H   10  CH7     2   ANG7     11  -120.   0
X   2   1.      1   90.      3   -120.   0
C   2   CN      1   ANG      3   -120.   0
H   15  CH6     2   ANG6     14  180.    0
H   15  CH7     2   ANG7     16  120.    0
H   15  CH7     2   ANG7     16  -120.   0
```

Variables:

CN	1.45524
ANG	108.31107
CH6	1.10391
ANG6	112.12778
CH7	1.08927
ANG7	109.58619

PYRROLE MP2/6-31+G(D,P) OPTIMIZED STRUCTURE

Symbolic Z-matrix:

Charge = 0 Multiplicity = 1

N							
H	1	NH					
C	1	NC3	2	ANG3			
C	1	NC3	2	ANG3	3	180.	0
C	3	CC5	1	ANG5	2	180.	0
C	4	CC5	1	ANG5	2	180.	0
H	3	CH7	1	ANG7	2	0.	0
H	4	CH7	1	ANG7	2	0.	0
H	5	CH9	3	ANG9	7	0.	0
H	6	CH9	4	ANG9	8	0.	0

Variables:

NH	1.00719
NC3	1.37454
ANG3	124.91284
CC5	1.38571
ANG5	107.39955
CH7	1.07699
ANG7	121.2349
CH9	1.07789
ANG9	125.5103

3,4-DIFLUOROPYRROLE MP2/6-31+G(D,P) OPTIMIZED STRUCTURE

Symbolic Z-matrix:

Charge = 0 Multiplicity = 1

N							
H	1	NH					
C	1	NC3	2	ANG3			
C	1	NC3	2	ANG3	3	180.	0
C	3	CC5	1	ANG5	2	180.	0
C	4	CC5	1	ANG5	2	180.	0
H	3	CH7	1	ANG7	2	0.	0
H	4	CH7	1	ANG7	2	0.	0
F	5	CF9	3	ANG9	7	0.	0
F	6	CF9	4	ANG9	8	0.	0

Variables:

NH	1.00642
NC3	1.37537
ANG3	124.35981
CC5	1.38271
ANG5	106.17897
CH7	1.07515
ANG7	122.98626
CF9	1.353
ANG9	126.09995

2,5-DIFLUOROPYRROLE MP2/6-31+G(D,P) OPTIMIZED STRUCTURE

Symbolic Z-matrix:

Charge = 0 Multiplicity = 1

N							
H	1	NH					
C	1	NC3	2	ANG3			
C	1	NC3	2	ANG3	3	180.	0
C	3	CC5	1	ANG5	2	180.	0
C	4	CC5	1	ANG5	2	180.	0
F	3	CH7	1	ANG7	2	0.	0
F	4	CH7	1	ANG7	2	0.	0
H	5	CF9	3	ANG9	7	0.	0
H	6	CF9	4	ANG9	8	0.	0

Variables:

NH	1.00822
NC3	1.37245
ANG3	126.57082
CC5	1.36933
ANG5	110.2977
CH7	1.34964
ANG7	118.43637
CF9	1.07588
ANG9	126.21828

2,5-DIBERYLLIUMPYRROLE^{+2} MP2/6-31+G(D,P) OPTIMIZED STRUCTURE

Symbolic Z-matrix:
Charge = 2 Multiplicity = 1

N							
H	1	NH					
C	1	NC3	2	ANG3			
C	1	NC3	2	ANG3	3	180.	0
C	3	CC5	1	ANG5	2	180.	0
C	4	CC5	1	ANG5	2	180.	0
Be	3	CB7	1	ANG7	2	0.	0
Be	4	CB7	1	ANG7	2	0.	0
H	5	CH9	3	ANG9	7	0.	0
H	6	CH9	4	ANG9	8	0.	0

Variables:

NH	1.01205
NC3	1.37986
ANG3	124.70633
CC5	1.41761
ANG5	106.80951
CB7	1.63453
ANG7	131.01899
CH9	1.08059
ANG9	126.42836

3,4-DIBERYLLIUMPYRROLE^{+2} MP2/6-31+G(D,P) OPTIMIZED STRUCTURE

Symbolic Z-matrix:
Charge = 2 Multiplicity = 1

N							
H	1	NH					
C	1	NC3	2	ANG3			
C	1	NC3	2	ANG3	3	180.	0
C	3	CC5	1	ANG5	2	180.	0
C	4	CC5	1	ANG5	2	180.	0
H	3	CH7	1	ANG7	2	0.	0
H	4	CH7	1	ANG7	2	0.	0
Be	5	CB9	3	ANG9	7	0.	0
Be	6	CB9	4	ANG9	8	0.	0

Variables:

NH	1.01704
NC3	1.35921
ANG3	124.71613
CC5	1.40565
ANG5	108.75509
CH7	1.08075
ANG7	120.15547
CB9	1.62595
ANG9	115.79211

Appendix 2

Z-matrices for optimized complexes reported in Tables 5 and 6, taken directly from Gaussian 98 output

---

PYRROLE:NCH MP2/6-31+G(D,P) OPTIMIZED STRUCTURE

Symbolic Z-matrix:
Charge = 0 Multiplicity = 1

```
N
H          1  NH
C          1  NC3    2  ANG3
C          1  NC3    2  ANG3    3   180.    0
C          3  CC5    1  ANG5    2   180.    0
C          4  CC5    1  ANG5    2   180.    0
H          3  CH7    1  ANG7    2   0.      0
H          4  CH7    1  ANG7    2   0.      0
H          5  CH9    3  ANG9    7   0.      0
H          6  CH9    4  ANG9    8   0.      0
X          1  1.     2  90.     3   0.      0
N          1  R      11 90.     2   0.      0
X          12 1.     1  90.     11  0.      0
C          12 CNC    13 90.     1   180.    0
X          14 1.     12 90.     13  0.      0
H          14 CHC    15 90.     12  180.    0
```

Variables:

NH	1.01145
NC3	1.37274
ANG3	125.0453
CC5	1.38729
ANG5	107.69096
CH7	1.0773
ANG7	121.10689
CH9	1.07817
ANG9	125.63111
R	3.16425
CNC	1.17684
CHC	1.06718

PYRROLE:NCLi MP2/6-31+G(D,P) OPTIMIZED STRUCTURE

Symbolic Z-matrix:
Charge = 0 Multiplicity = 1

```
N
H              1  NH
C              1  NC3    2  ANG3
C              1  NC3    2  ANG3    3   180.    0
C              3  CC5    1  ANG5    2   180.    0
C              4  CC5    1  ANG5    2   180.    0
H              3  CH7    1  ANG7    2   0.      0
H              4  CH7    1  ANG7    2   0.      0
H              5  CH9    3  ANG9    7   0.      0
H              6  CH9    4  ANG9    8   0.      0
X              1  1.     2  90.     3   0.      0
N              1  R      11 90.     2   0.      0
X              12 1.     1  90.     11  0.      0
C              12 CN     13 90.     2   180.    0
X              14 1.     12 90.     13  0.      0
Li             14 CLi    15 90.     12  180.    0
```

Variables:

NH	1.01918
NC3	1.37077
ANG3	125.1347
CC5	1.38902
ANG5	107.92298
CH7	1.07748
ANG7	120.94505
CH9	1.0785
ANG9	125.73911
R	3.00996
CN	1.19037
CLi	1.95756

PYRROLE:NCNa MP2/6-31+G(D,P) OPTIMIZED STRUCTURE WITH ONLY THE 1s ORBITALS FROZEN

Symbolic Z-matrix:
Charge = 0 Multiplicity = 1

```
N
H          1  NH
C          1  NC3    2  ANG3
C          1  NC3    2  ANG3    3   180.    0
C          3  CC5    1  ANG5    2   180.    0
C          4  CC5    1  ANG5    2   180.    0
H          3  CH7    1  ANG7    2   0.      0
H          4  CH7    1  ANG7    2   0.      0
H          5  CH9    3  ANG9    7   0.      0
H          6  CH9    4  ANG9    8   0.      0
X          1  1.     2  90.     3   0.      0
N          1  R      11 90.     2   0.      0
X          12 1.     1  90.     11  0.      0
C          12 CN     13 90.     2   180.    0
X          14 1.     12 90.     13  0.      0
Na         14 CNa    15 90.     12  180.    0
```

Variables:

NH	1.02136
NC3	1.37017
ANG3	125.15207
CC5	1.38941
ANG5	107.97728
CH7	1.07754
ANG7	120.90459
CH9	1.07859
ANG9	125.76743
R	2.97113
CN	1.19061
CNa	2.2352

PYRROLE:NCS^- MP2/6-31+G(D,P) OPTIMIZED STRUCTURE

Symbolic Z-matrix:
Charge = -1 Multiplicity = 1

```
N
H          1  NH
C          1  NC3    2  ANG3
C          1  NC3    2  ANG3    3  180.    0
C          3  CC5    1  ANG5    2  180.    0
C          4  CC5    1  ANG5    2  180.    0
H          3  CH7    1  ANG7    2  0.      0
H          4  CH7    1  ANG7    2  0.      0
H          5  CH9    3  ANG9    7  0.      0
H          6  CH9    4  ANG9    8  0.      0
X          1  1.     2  90.     3  0.      0
N          1  R      11 90.     2  0.      0
X          12 1.     1  90.     11 0.      0
C          12 CN     13 90.     2  180.    0
X          14 1.     12 90.     13 0.      0
S          14 CS     15 90.     12 180.    0
```

Variables:

NH	1.03697
NC3	1.36755
ANG3	125.23316
CC5	1.39197
ANG5	108.24055
CH7	1.07777
ANG7	120.65796
CH9	1.07931
ANG9	125.86253
R	2.83533
CN	1.20192
CS	1.64653

PYRROLE:NCO^- MP2/6-31+G(D,P) OPTIMIZED STRUCTURE

Symbolic Z-matrix:
Charge = -1 Multiplicity = 1

```
N
H          1  NH
C          1  NC3    2  ANG3
C          1  NC3    2  ANG3    3   180.    0
C          3  CC5    1  ANG5    2   180.    0
C          4  CC5    1  ANG5    2   180.    0
H          3  CH7    1  ANG7    2   0.      0
H          4  CH7    1  ANG7    2   0.      0
H          5  CH9    3  ANG9    7   0.      0
H          6  CH9    4  ANG9    8   0.      0
X          1  1.     2  90.     3   0.      0
N          1  R      11 90.     2   0.      0
X          12 1.     1  90.     11  90.     0
C          12 CN     13 90.     2   180.    0
X          14 1.     12 90.     13  90.     0
O          14 CO     15 90.     12  180.    0
```

Variables:

NH	1.04842
NC3	1.36662
ANG3	125.32201
CC5	1.39319
ANG5	108.43029
CH7	1.078
ANG7	120.5426
CH9	1.07963
ANG9	125.95387
R	2.76188
CN	1.21103
CO	1.23307

3,4-DIFLUOROPYRROLE:NCH MP2/6-31+G(D,P) OPTIMIZED STRUCTURE

Symbolic Z-matrix:
Charge = 0 Multiplicity = 1

```
N
H          1  NH
C          1  NC3    2  ANG3
C          1  NC3    2  ANG3    3   180.    0
C          3  CC5    1  ANG5    2   180.    0
C          4  CC5    1  ANG5    2   180.    0
H          3  CH7    1  ANG7    2   0.      0
H          4  CH7    1  ANG7    2   0.      0
F          5  CF9    3  ANG9    7   0.      0
F          6  CF9    4  ANG9    8   0.      0
X          1  1.     2  90.     3   0.      0
N          1  R      11 90.     2   0.      0
X          12 1.     1  90.     11  90.     0
C          12 CN     13 90.     2   180.    0
X          14 1.     12 90.     13  0.      0
H          14 CH     15 90.     12  180.    0
```

Variables:

NH	1.01197
NC3	1.37354
ANG3	124.47348
CC5	1.38394
ANG5	106.42129
CH7	1.07534
ANG7	122.7922
CF9	1.35565
ANG9	126.22311
R	3.11482
CN	1.17644
CH	1.06735

3,4-DIFLUOROPYRROLE:NCLi MP2/6-31+G(D,P) OPTIMIZED STRUCTURE

Symbolic Z-matrix:
Charge = 0 Multiplicity = 1

```
N
H          1  NH
C          1  NC3    2  ANG3
C          1  NC3    2  ANG3    3   180.    0
C          3  CC5    1  ANG5    2   180.    0
C          4  CC5    1  ANG5    2   180.    0
H          3  CH7    1  ANG7    2   0.      0
H          4  CH7    1  ANG7    2   0.      0
F          5  CF9    3  ANG9    7   0.      0
F          6  CF9    4  ANG9    8   0.      0
X          1  1.     2  90.     3   0.      0
N          1  R      11 90.     2   0.      0
X          12 1.     1  90.     11  0.      0
C          12 CN     13 90.     2   180.    0
X          14 1.     12 90.     13  0.      0
Li         14 CLi    15 90.     12  180.    0
```

Variables:

NH	1.02162
NC3	1.37164
ANG3	124.561
CC5	1.38518
ANG5	106.624
CH7	1.07546
ANG7	122.603
CF9	1.35875
ANG9	126.302
R	2.95558
CN	1.18991
CLi	1.96118

3,4-DIFLUOROPYRROLE:NCNa MP2/6-31+G(D,P) OPTIMIZED STRUCTURE WITH ONLY THE 1s ORBITALS FROZEN

Symbolic Z-matrix:
Charge = 0 Multiplicity = 1

```
N
H              1   NH
C              1   NC3     2   ANG3
C              1   NC3     2   ANG3     3    180.    0
C              3   CC5     1   ANG5     2    180.    0
C              4   CC5     1   ANG5     2    180.    0
H              3   CH7     1   ANG7     2    0.      0
H              4   CH7     1   ANG7     2    0.      0
F              5   CF9     3   ANG9     7    0.      0
F              6   CF9     4   ANG9     8    0.      0
X              1   1.      2   90.      3    0.      0
N              1   R      11   90.      2    0.      0
X             12   1.      1   90.     11    0.      0
C             12   CN     13   90.      2    180.    0
X             14   1.     12   90.     13    0.      0
Na            14   CNa    15   90.     12    180.    0
```

Variables:

NH	1.02453
NC3	1.37101
ANG3	124.58235
CC5	1.38554
ANG5	106.68114
CH7	1.0755
ANG7	122.54787
CF9	1.35956
ANG9	126.32501
R	2.91624
CN	1.19013
CNa	2.23883

3,4-DIFLUOROPYRROLE:NCS^- MP2/6-31+G(D,P) OPTIMIZED STRUCTURE

Symbolic Z-matrix:
Charge = -1 Multiplicity = 1

```
N
H          1  NH
C          1  NC3    2  ANG3
C          1  NC3    2  ANG3    3   180.    0
C          3  CC5    1  ANG5    2   180.    0
C          4  CC5    1  ANG5    2   180.    0
H          3  CH7    1  ANG7    2   0.      0
H          4  CH7    1  ANG7    2   0.      0
F          5  CF9    3  ANG9    7   0.      0
F          6  CF9    4  ANG9    8   0.      0
X          1  1.     2  90.     3   0.      0
N          1  R      11 90.     2   0.      0
X          12 1.     1  90.     11  90.     0
C          12 CN     13 90.     2   180.    0
X          14 1.     12 90.     13  90.     0
S          14 CS     15 90.     12  180.    0
```

Variables:

NH	1.04549
NC3	1.36861
ANG3	124.6613
CC5	1.38743
ANG5	106.88917
CH7	1.07576
ANG7	122.24548
CF9	1.36603
ANG9	126.50156
R	2.77007
CN	1.20183
CS	1.64283

3,4-DIFLUOROPYRROLE:NCO^- MP2/6-31+G(D,P) OPTIMIZED STRUCTURE

Symbolic Z-matrix:
Charge = -1 Multiplicity = 1

```
N
H          1  NH
C          1  NC3    2  ANG3
C          1  NC3    2  ANG3    3   180.   0
C          3  CC5    1  ANG5    2   180.   0
C          4  CC5    1  ANG5    2   180.   0
H          3  CH7    1  ANG7    2   0.     0
H          4  CH7    1  ANG7    2   0.     0
F          5  CF9    3  ANG9    7   0.     0
F          6  CF9    4  ANG9    8   0.     0
X          1  1.     2  90.     3   0.     0
N          1  R      11 90.     2   0.     0
X          12 1.     1  90.     11  90.    0
C          12 CN     13 90.     2   180.   0
X          14 1.     12 90.     13  90.    0
O          14 CO     15 90.     12  180.   0
```

Variables:

NH	1.06116
NC3	1.36779
ANG3	124.74926
CC5	1.38839
ANG5	107.05874
CH7	1.07595
ANG7	122.11971
CF9	1.36825
ANG9	126.58183
R	2.69898
CN	1.21034
CO	1.2305

2,5-DIFLUOROPYRROLE:NCH MP2/6-31+G(D,P) OPTIMIZED STRUCTURE

Symbolic Z-matrix:
Charge = 0 Multiplicity = 1

```
N
H          1  NH
C          1  NC3    2  ANG3
C          1  NC3    2  ANG3    3   180.    0
C          3  CC5    1  ANG5    2   180.    0
C          4  CC5    1  ANG5    2   180.    0
F          3  CF7    1  ANG7    2   0.      0
F          4  CF7    1  ANG7    2   0.      0
H          5  CH9    3  ANG9    7   0.      0
H          6  CH9    4  ANG9    8   0.      0
X          1  1.     2  90.     3   0.      0
N          1  R      11 90.     2   0.      0
X          12 1.     1  90.     11  90.     0
C          12 CN     13 90.     2   180.    0
X          14 1.     12 90.     13  0.      0
H          14 CH     15 90.     12  180.    0
```

Variables:

NH	1.01597
NC3	1.36978
ANG3	126.75778
CC5	1.3709
ANG5	110.70464
CF7	1.35217
ANG7	118.57975
CH9	1.07602
ANG9	126.3571
R	3.06836
CN	1.17607
CH	1.06723

2,5-DIFLUOROPYRROLE:NCLi MP2/6-31+G(D,P) OPTIMIZED STRUCTURE

Symbolic Z-matrix:
Charge = 0 Multiplicity = 1

```
N
H          1  NH
C          1  NC3    2  ANG3
C          1  NC3    2  ANG3    3   180.   0
C          3  CC5    1  ANG5    2   180.   0
C          4  CC5    1  ANG5    2   180.   0
F          3  CF7    1  ANG7    2   0.     0
F          4  CF7    1  ANG7    2   0.     0
H          5  CH9    3  ANG9    7   0.     0
H          6  CH9    4  ANG9    8   0.     0
X          1  1.     2  90.     3   0.     0
N          1  R      11 90.     2   0.     0
X          12 1.     1  90.     11  90.    0
C          12 CN     13 90.     2   180.   0
X          14 1.     12 90.     13  0.     0
Li         14 CLi    15 90.     12  180.   0
```

Variables:

NH	1.02908
NC3	1.36752
ANG3	126.896
CC5	1.37259
ANG5	111.015
CF7	1.35387
ANG7	118.831
CH9	1.07619
ANG9	126.437
R	2.90552
CN	1.18942
CLi	1.9598

2,5-DIFLUOROPYRROLE:NCNa MP2/6-31+G(D,P) OPTIMIZED STRUCTURE WITH ONLY THE 1s ORBITALS FROZEN

Symbolic Z-matrix:
Charge = 0 Multiplicity = 1

```
N
H          1  NH
C          1  NC3    2  ANG3
C          1  NC3    2  ANG3    3   180.    0
C          3  CC5    1  ANG5    2   180.    0
C          4  CC5    1  ANG5    2   180.    0
F          3  CF7    1  ANG7    2   0.      0
F          4  CF7    1  ANG7    2   0.      0
H          5  CH9    3  ANG9    7   0.      0
H          6  CH9    4  ANG9    8   0.      0
X          1  1.     2  90.     3   0.      0
N          1  R      11 90.     2   0.      0
X          12 1.     1  90.     11  0.      0
C          12 CN     13 90.     2   180.    0
X          14 1.     12 90.     13  0.      0
Na         14 CNa    15 90.     12  180.    0
```

Variables:

NH	1.03329
NC3	1.36672
ANG3	126.93282
CC5	1.37298
ANG5	111.10681
CF7	1.35445
ANG7	118.88337
CH9	1.07624
ANG9	126.46172
R	2.86275
CN	1.18956
CNa	2.236

2,5-DIFLUOROPYRROLE:NCS^- MP2/6-31+G(D,P) OPTIMIZED STRUCTURE

Symbolic Z-matrix:
Charge = -1 Multiplicity = 1

```
N
H          1  NH
C          1  NC3    2  ANG3
C          1  NC3    2  ANG3    3  180.    0
C          3  CC5    1  ANG5    2  180.    0
C          4  CC5    1  ANG5    2  180.    0
F          3  CF7    1  ANG7    2  0.      0
F          4  CF7    1  ANG7    2  0.      0
H          5  CH9    3  ANG9    7  0.      0
H          6  CH9    4  ANG9    8  0.      0
X          1  1.     2  90.     3  0.      0
N          1  R      11 90.     2  0.      0
X          12 1.     1  90.     11 0.      0
C          12 CN     13 90.     2  180.    0
X          14 1.     12 90.     13 0.      0
S          14 CS     15 90.     12 180.    0
```

Variables:

NH	1.06469
NC3	1.36385
ANG3	127.16137
CC5	1.37605
ANG5	111.59723
CF7	1.35582
ANG7	119.32725
CH9	1.07672
ANG9	126.49287
R	2.71255
CN	1.20091
CS	1.64206

2,5-DIFLUOROPYRROLE:NCO^- MP2/6-31+G(D,P) OPTIMIZED STRUCTURE

Symbolic Z-matrix:
Charge = -1 Multiplicity = 1

```
N
H          1  NH
C          1  NC3    2  ANG3
C          1  NC3    2  ANG3    3   180.    0
C          3  CC5    1  ANG5    2   180.    0
C          4  CC5    1  ANG5    2   180.    0
F          3  CF7    1  ANG7    2   0.      0
F          4  CF7    1  ANG7    2   0.      0
H          5  CH9    3  ANG9    7   0.      0
H          6  CH9    4  ANG9    8   0.      0
X          1  1.     2  90.     3   0.      0
N          1  R     11  90.     2   0.      0
X         12  1.     1  90.    11   90.     0
C         12  CN    13  90.     2   180.    0
X         14  1.    12  90.    13   90.     0
O         14  CO    15  90.    12   180.    0
```

Variables:

NH	1.09727
NC3	1.36218
ANG3	127.3628
CC5	1.37767
ANG5	111.99689
CF7	1.35866
ANG7	119.41544
CH9	1.07702
ANG9	126.60676
R	2.62714
CN	1.20816
CO	1.22899

3,4-DIBERYLLIUMPYRROLE^{+2}:NCH MP2/6-31+G(D,P) OPTIMIZED STRUCTURE

Symbolic Z-matrix:
Charge = 2 Multiplicity = 1

```
N
H          1  NH
C          1  NC3    2  ANG3
C          1  NC3    2  ANG3    3   180.    0
C          3  CC5    1  ANG5    2   180.    0
C          4  CC5    1  ANG5    2   180.    0
H          3  CH7    1  ANG7    2   0.      0
H          4  CH7    1  ANG7    2   0.      0
Be         5  CB9    3  ANG9    7   0.      0
Be         6  CB9    4  ANG9    8   0.      0
X          1  1.     2  90.     3   0.      0
N          1  R      11 90.     2   0.      0
X          12 1.     1  90.     11  90.     0
C          12 CN     13 90.     2   180.    0
X          14 1.     12 90.     13  0.      0
H          14 CH     15 90.     12  180.    0
```

Variables:

NH	1.04261
NC3	1.3562
ANG3	124.97802
CC5	1.40873
ANG5	109.27251
CH7	1.08096
ANG7	120.01148
CB9	1.61987
ANG9	115.86886
R	2.82797
CN	1.17367
CH	1.07127

3,4-DIBERYLLIUMPYRROLE^{+2}:NCLi MP2/6-31+G(D,P) OPTIMIZED STRUCTURE

Symbolic Z-matrix:
Charge = 2 Multiplicity = 1

N							
H	1	NH					
C	1	NC3	2	ANG3			
C	1	NC3	2	ANG3	3	180.	0
C	3	CC5	1	ANG5	2	180.	0
C	4	CC5	1	ANG5	2	180.	0
H	3	CH7	1	ANG7	2	0.	0
H	4	CH7	1	ANG7	2	0.	0
Be	5	CB9	3	ANG9	7	0.	0
Be	6	CB9	4	ANG9	8	0.	0
X	1	1.	2	90.	3	0.	0
N	1	R	11	90.	2	0.	0
X	12	1.	1	90.	11	0.	0
C	12	CN	13	90.	2	180.	0
X	14	1.	12	90.	13	0.	0
Li	14	CLi	15	90.	12	180.	0

Variables:

NH	1.119
NC3	1.35389
ANG3	125.36541
CC5	1.41281
ANG5	109.9593
CH7	1.08143
ANG7	119.86253
CB9	1.61305
ANG9	115.84257
R	2.60336
CN	1.1865
CLi	2.03465

3,4-DIBERYLLIUMPYRROLE^{+2}:NCNa MP2/6-31+G(D,P) OPTIMIZED STRUCTURE WITH ONLY THE 1s ORBITALS FROZEN

Symbolic Z-matrix:
Charge = 2 Multiplicity = 1

```
N
H          1  NH
C          1  NC3    2  ANG3
C          1  NC3    2  ANG3    3  180.    0
C          3  CC5    1  ANG5    2  180.    0
C          4  CC5    1  ANG5    2  180.    0
H          3  CH7    1  ANG7    2  0.      0
H          4  CH7    1  ANG7    2  0.      0
Be         5  CB9    3  ANG9    7  0.      0
Be         6  CB9    4  ANG9    8  0.      0
X          1  1.     2  90.     3  0.      0
N          1  R      11 90.     2  0.      0
X          12 1.     1  90.     11 0.      0
C          12 CN     13 90.     2  180.    0
X          14 1.     12 90.     13 0.      0
Na         14 CNa    15 90.     12 180.    0
```

Variables:

NH	1.57739
NC3	1.35632
ANG3	126.58773
CC5	1.41964
ANG5	111.81214
CH7	1.08261
ANG7	120.05359
CB9	1.60544
ANG9	116.69726
R	2.66562
CN	1.17928
CNa	2.37425

PYRROLE:NH_3 MP2/6-31+G(D,P) OPTIMIZED STRUCTURE WITH N-H IN THE PLANE OF PYRROLE

Symbolic Z-matrix:
Charge = 0 Multiplicity = 1

```
N
H          1  NH
C          1  NC3    2  ANG3
C          1  NC3    2  ANG3    3   180.    0
C          3  CC5    1  ANG5    2   180.    0
C          4  CC5    1  ANG5    2   180.    0
H          3  CH7    1  ANG7    2   0.      0
H          4  CH7    1  ANG7    2   0.      0
H          5  CH9    3  ANG9    7   0.      0
H          6  CH9    4  ANG9    8   0.      0
X          1  1.     2  90.     3   0.      0
N          1  R      11 90.     2   0.      0
H          12 NH13   1  ANG13   11  0.      0
H          12 NH13   1  ANG13   13  120.    0
H          12 NH13   1  ANG13   13  -120.   0
```

Variables:

NH	1.02051
NC3	1.37221
ANG3	125.17681
CC5	1.38816
ANG5	107.92035
CH7	1.07762
ANG7	121.09502
CH9	1.07829
ANG9	125.71059
R	3.03747
NH13	1.01419
ANG13	111.87013

3,4-DIFLUOROPYRRROLE:NH_3 MP2/6-31+G(D,P) OPTIMIZED STRUCTURE WITH N-H IN THE PLANE OF PYRROLE

Symbolic Z-matrix:
Charge = 0 Multiplicity = 1

```
N
H          1  NH
C          1  NC3    2  ANG3
C          1  NC3    2  ANG3    3   180.    0
C          3  CC5    1  ANG5    2   180.    0
C          4  CC5    1  ANG5    2   180.    0
H          3  CH7    1  ANG7    2   0.      0
H          4  CH7    1  ANG7    2   0.      0
F          5  CF9    3  ANG9    7   0.      0
F          6  CF9    4  ANG9    8   0.      0
X          1  1.     2  90.     3   0.      0
N          1  R      11 90.     2   0.      0
H          12 NH13   1  ANG13   11  0.      0
X          12 1.     1  ANG14   13  180.    0
H          12 NH15   14 HALF    2   90.     0
H          12 NH15   14 HALF    2   -90.    0
```

Variables:

NH	1.02315
NC3	1.37312
ANG3	124.61556
CC5	1.3846
ANG5	106.65671
CH7	1.0756
ANG7	122.7817
CF9	1.35641
ANG9	126.26573
R	2.99166
NH13	1.01442
ANG13	111.0618
ANG14	129.79508
NH15	1.01426
HALF	53.52968

PYRROLE:$N(CH_3)_3$ MP2/6-31+G(D,P) OPTIMIZED STRUCTURE WITH C-H IN THE PLANE OF PYRROLE

Symbolic Z-matrix:
Charge = 0 Multiplicity = 1

```
N
H          1  NH
C          1  NC3    2  ANG3
C          1  NC3    2  ANG3    3   180.    0
C          3  CC5    1  ANG5    2   180.    0
C          4  CC5    1  ANG5    2   180.    0
H          3  CH7    1  ANG7    2   0.      0
H          4  CH7    1  ANG7    2   0.      0
H          5  CH9    3  ANG9    7   0.      0
H          6  CH9    4  ANG9    8   0.      0
X          1  1.     2  90.     3   0.      0
N          1  R      11 90.     2   0.      0
C          12 CN13   1  ANG13   11  0.      0
H          13 CH14   12 ANG14   2   180.    0
H          13 CH15   12 ANG15   14  120.    0
H          13 CH15   12 ANG15   14  -120.   0
X          12 1.     1  90.     11  120.    0
C          12 CN13   1  ANG13   11  120.    0
H          18 CH14   12 ANG14   17  180.    0
H          18 CH15   12 ANG15   19  120.    0
H          18 CH15   12 ANG15   19  -120.   0
X          12 1.     1  90.     11  -120.   0
C          12 CN13   1  ANG13   11  -120.   0
H          23 CH14   12 ANG14   22  180.    0
H          23 CH15   12 ANG15   24  120.    0
H          23 CH15   12 ANG15   24  -120.   0
```

Variables:

NH	1.02932
NC3	1.37262
ANG3	125.23777
CC5	1.38864
ANG5	108.00819
CH7	1.07797
ANG7	121.09147
CH9	1.0784
ANG9	125.74811
R	2.93063
CN13	1.46104

ANG13	108.27578
CH14	1.10083
ANG14	111.72914
CH15	1.08932
ANG15	109.51702

2,5-DIFLUOROPYRROLE:NH_3 MP2/6-31+G(D,P) OPTIMIZED STRUCTURE WITH N-H IN THE PLANE OF PYRROLE

Symbolic Z-matrix:
Charge = 0 Multiplicity = 1

```
N
H          1  NH
C          1  NC3    2  ANG3
C          1  NC3    2  ANG3    3   180.    0
C          3  CC5    1  ANG5    2   180.    0
C          4  CC5    1  ANG5    2   180.    0
F          3  CF7    1  ANG7    2   0.      0
F          4  CF7    1  ANG7    2   0.      0
H          5  CH9    3  ANG9    7   0.      0
H          6  CH9    4  ANG9    8   0.      0
X          1  1.     2  90.     3   0.      0
N          1  R      11 90.     2   0.      0
H          12 NH13   1  ANG13   11  0.      0
X          12 1.     1  ANG14   13  180.    0
H          12 NH15   14 HALF    2   90.     0
H          12 NH15   14 HALF    2   -90.    0
```

Variables:

NH	1.03199
NC3	1.36824
ANG3	126.91867
CC5	1.37175
ANG5	111.02601
CF7	1.35493
ANG7	118.46533
CH9	1.07611
ANG9	126.49143
R	2.92369
NH13	1.01461
ANG13	110.77965
ANG14	129.57577
NH15	1.01432
HALF	53.52718

3,4-DIFLUOROPYRROLE:$N(CH_3)_3$ MP2/6-31+G(D,P) OPTIMIZED STRUCTURE WITH C-H IN THE PLANE OF PYRROLE

Symbolic Z-matrix:
Charge = 0 Multiplicity = 1

```
N
H              1  NH
C              1  NC3    2  ANG3
C              1  NC3    2  ANG3    3   180.    0
C              3  CC5    1  ANG5    2   180.    0
C              4  CC5    1  ANG5    2   180.    0
H              3  CH7    1  ANG7    2   0.      0
H              4  CH7    1  ANG7    2   0.      0
F              5  CF9    3  ANG9    7   0.      0
F              6  CF9    4  ANG9    8   0.      0
X              1  1.     2  90.     3   0.      0
N              1  R      11  90.     2   0.      0
C             12  CN13    1  ANG13   11   0.      0
H             13  CH14   12  ANG14    2   180.    0
H             13  CH15   12  ANG15   14   120.    0
H             13  CH15   12  ANG15   14  -120.    0
X             12  1.      1  90.     11   120.    0
C             12  CN13    1  ANG13   11   120.    0
H             18  CH14   12  ANG14   17   180.    0
H             18  CH15   12  ANG15   19   120.    0
H             18  CH15   12  ANG15   19  -120.    0
X             12  1.      1  90.     11  -120.    0
C             12  CN13    1  ANG13   11  -120.    0
H             23  CH14   12  ANG14   22   180.    0
H             23  CH15   12  ANG15   24   120.    0
H             23  CH15   12  ANG15   24  -120.    0
```

Variables:

NH	1.03483
NC3	1.37355
ANG3	124.68895
CC5	1.38506
ANG5	106.76203
CH7	1.07593
ANG7	122.76846
CF9	1.35665
ANG9	126.31675
R	2.8813
CN13	1.4626

ANG13	108.36704
CH14	1.10006
ANG14	111.64753
CH15	1.08929
ANG15	109.51161

2,5-DIBERYLLIUMPYRROLE^{+2}:NH_3 MP2/6-31+G(D,P) OPTIMIZED STRUCTURE WITH N-H IN THE PLANE OF PYRROLE

Symbolic Z-matrix:
Charge = 2 Multiplicity = 1

```
N
H          1  NH
C          1  NC3    2  ANG3
C          1  NC3    2  ANG3    3   180.    0
C          3  CC5    1  ANG5    2   180.    0
C          4  CC5    1  ANG5    2   180.    0
Be         3  CB7    1  ANG7    2   0.      0
Be         4  CB7    1  ANG7    2   0.      0
H          5  CH9    3  ANG9    7   0.      0
H          6  CH9    4  ANG9    8   0.      0
X          1  1.     2  90.     3   0.      0
N          1  R      11 90.     2   0.      0
H          12 NH13   1  ANG13   11  0.      0
X          12 1.     1  ANG14   13  180.    0
H          12 NH15   14 HALF    2   90.     0
H          12 NH15   14 HALF    2   -90.    0
```

Variables:

NH	1.04998
NC3	1.37678
ANG3	125.29748
CC5	1.42237
ANG5	107.8302
CB7	1.62835
ANG7	130.43711
CH9	1.08061
ANG9	126.61663
R	2.86999
NH13	1.0177
ANG13	114.61623
ANG14	131.06211
NH15	1.01801
HALF	52.84008

2,5-DIFLUOROPYRROLE:$N(CH_3)_3$ MP2/6-31+G(D,P) OPTIMIZED STRUCTURE WITH C-H IN THE PLANE OF PYRROLE

Symbolic Z-matrix:
Charge = 0 Multiplicity = 1

```
N
H            1  NH
C            1  NC3    2  ANG3
C            1  NC3    2  ANG3    3   180.    0
C            3  CC5    1  ANG5    2   180.    0
C            4  CC5    1  ANG5    2   180.    0
F            3  CF7    1  ANG7    2   0.      0
F            4  CF7    1  ANG7    2   0.      0
H            5  CH9    3  ANG9    7   0.      0
H            6  CH9    4  ANG9    8   0.      0
X            1  1.     2  90.     3   0.      0
N            1  R      11 90.     2   0.      0
C            12 CN13   1  ANG13   11  0.      0
H            13 CH14   12 ANG14   2   180.    0
H            13 CH15   12 ANG15   14  120.    0
H            13 CH15   12 ANG15   14  -120.   0
X            12 1.     1  90.     11  120.    0
C            12 CN13   1  ANG13   11  120.    0
H            18 CH14   12 ANG14   17  180.    0
H            18 CH15   12 ANG15   19  120.    0
H            18 CH15   12 ANG15   19  -120.   0
X            12 1.     1  90.     11  -120.   0
C            12 CN13   1  ANG13   11  -120.   0
H            23 CH14   12 ANG14   22  180.    0
H            23 CH15   12 ANG15   24  120.    0
H            23 CH15   12 ANG15   24  -120.   0
```

Variables:

NH	1.05382
NC3	1.36713
ANG3	127.03289
CC5	1.37264
ANG5	111.26767
CF7	1.35739
ANG7	118.25659
CH9	1.07629
ANG9	126.63561
R	2.78489
CN13	1.46348

ANG13	108.09165
CH14	1.09938
ANG14	111.45819
CH15	1.08913
ANG15	109.45257

3,4-DIBERYLLIUMPYRROLE^{+2}:NH_3 MP2/6-31+G(D,P) OPTIMIZED STRUCTURE WITH N-H IN THE PLANE OF PYRROLE

Symbolic Z-matrix:
Charge = 2 Multiplicity = 1

```
N
H          1  NH
C          1  NC3    2  ANG3
C          1  NC3    2  ANG3    3   180.    0
C          3  CC5    1  ANG5    2   180.    0
C          4  CC5    1  ANG5    2   180.    0
H          3  CH7    1  ANG7    2   0.      0
H          4  CH7    1  ANG7    2   0.      0
Be         5  CB9    3  ANG9    7   0.      0
Be         6  CB9    4  ANG9    8   0.      0
X          1  1.     2  90.     3   0.      0
N          1  R      11 90.     2   0.      0
H          12 NH13   1  ANG13   11  0.      0
X          12 1.     1  ANG14   13  180.    0
H          12 NH15   14 HALF    2   90.     0
H          12 NH15   14 HALF    2   -90.    0
```

Variables:

NH	1.10749
NC3	1.35665
ANG3	125.38834
CC5	1.4108
ANG5	109.89971
CH7	1.08129
ANG7	120.10222
CB9	1.61813
ANG9	116.27728
R	2.69776
NH13	1.01801
ANG13	112.89233
ANG14	130.52483
NH15	1.01797
HALF	53.01118

2,5-DIBERYLLIUMPYRROLE^{+2}:N$(CH_3)_3$ MP2/6-31+G(D,P) OPTIMIZED STRUCTURE WITH C-H IN THE PLANE OF PYRROLE

Symbolic Z-matrix:
Charge = 2 Multiplicity = 1

```
N
H          1  NH
C          1  NC3    2  ANG3
C          1  NC3    2  ANG3    3   180.    0
C          3  CC5    1  ANG5    2   180.    0
C          4  CC5    1  ANG5    2   180.    0
Be         3  CB7    1  ANG7    2    0.     0
Be         4  CB7    1  ANG7    2    0.     0
H          5  CH9    3  ANG9    7    0.     0
H          6  CH9    4  ANG9    8    0.     0
X          1  1.     2  90.     3    0.     0
N          1  R     11  90.     2    0.     0
C         12  CN13   1  ANG13  11    0.     0
H         13  CH14  12  ANG14   2   180.    0
H         13  CH15  12  ANG15  14   120.    0
H         13  CH15  12  ANG15  14  -120.    0
X         12  1.     1  90.    11   120.    0
C         12  CN13   1  ANG13  11   120.    0
H         18  CH14  12  ANG14  17   180.    0
H         18  CH15  12  ANG15  19   120.    0
H         18  CH15  12  ANG15  19  -120.    0
X         12  1.     1  90.    11  -120.    0
C         12  CN13   1  ANG13  11  -120.    0
H         23  CH14  12  ANG14  22   180.    0
H         23  CH15  12  ANG15  24   120.    0
H         23  CH15  12  ANG15  24  -120.    0
```

Variables:

NH	1.7733
NC3	1.3807
ANG3	127.90116
CC5	1.4362
ANG5	111.91469
CB7	1.61848
ANG7	136.72016
CH9	1.08299
ANG9	127.8354
R	2.83734
CN13	1.49175

ANG13	107.80266
CH14	1.08759
ANG14	109.19568
CH15	1.08662
ANG15	108.75663

3,4-DIBERYLLIUMPYRROLE^{+2}:N$(CH_3)_3$ MP2/6-31+G(D,P) OPTIMIZED STRUCTURE WITH C-H IN THE PLANE OF PYRROLE

Symbolic Z-matrix:
Charge = 2 Multiplicity = 1

```
N
H          1  NH
C          1  NC3    2  ANG3
C          1  NC3    2  ANG3    3   180.    0
C          3  CC5    1  ANG5    2   180.    0
C          4  CC5    1  ANG5    2   180.    0
H          3  CH7    1  ANG7    2   0.      0
H          4  CH7    1  ANG7    2   0.      0
Be         5  CB9    3  ANG9    7   0.      0
Be         6  CB9    4  ANG9    8   0.      0
X          1  1.     2  90.     3   0.      0
N          1  R      11 90.     2   0.      0
C          12 CN13   1  ANG13   11  0.      0
H          13 CH14   12 ANG14   2   180.    0
H          13 CH15   12 ANG15   14  120.    0
H          13 CH15   12 ANG15   14  -120.   0
X          12 1.     1  90.     11  120.    0
C          12 CN13   1  ANG13   11  120.    0
H          18 CH14   12 ANG14   17  180.    0
H          18 CH15   12 ANG15   19  120.    0
H          18 CH15   12 ANG15   19  -120.   0
X          12 1.     1  90.     11  -120.   0
C          12 CN13   1  ANG13   11  -120.   0
H          23 CH14   12 ANG14   22  180.    0
H          23 CH15   12 ANG15   24  120.    0
H          23 CH15   12 ANG15   24  -120.   0
```

Variables:

NH	1.82163
NC3	1.35924
ANG3	126.9271
CC5	1.42016
ANG5	112.26277
CH7	1.08281
ANG7	120.23648
CB9	1.60752
ANG9	117.53224
R	2.87458
CN13	1.49239

ANG13	107.51908
CH14	1.08738
ANG14	108.92436
CH15	1.0864
ANG15	108.73134

Appendix 3

Binding Enthalpies (ΔH^0) for complexes in Tables 5 and 6

Binding Enthalpies (kcal/mol)

	Py[a]	3,4-diFPy	2,5-diFPy	2,5-diBePy^{+2}	3,4-diBePy^{+2}
NCH	-4.5	-5.6	-5.7	- - -	-20.2
NCLi	-9.3	-11.7	-11.6	- - -	-47.2
NCNa	-10.7	-13.5	-13.3	- - -	-55.8
NCS^-	-18.1	-23.7	-21.7	- - -	- - -
NCO^-	-22.0	-28.6	-27.2	- - -	- - -
NH_3	-7.0	-8.4	-9.6	-21.4	-25.4
$N(CH_3)_3$	-9.4	-11.0	-13.3	-32.6	-44.8

a) Py=pyrrole